

## Award Accounts

The Chemical Society of Japan Award for Creative Work for 2008

# Construction of Cooperative and Responsive Supramolecular Systems for Molecular Functional Modulation

Tatsuya Nabeshima

Graduate School of Pure and Applied Sciences, University of Tsukuba, Tsukuba 305-8571

Received January 22, 2010; E-mail: nabesima@chem.tsukuba.ac.jp

The transfer and modulation of the molecular information are necessary processes for cooperative and responsive molecular functions. When functional molecules are responsive to external (intermolecular) as well as internal (intramolecular) stimuli, the molecules exhibit cooperative functions in principle. We have developed a variety of cooperative and responsive supramolecular systems created on the basis of new concepts for the molecular design of sophisticated functional systems. The first uses pseudomacrocycles including pseudocrown ether, pseudocryptands, and pseudocyclophanes as novel frameworks for response functions by utilizing a metal ion as an effector. The second utilizes a molecular gate responding to an external signal. The gate is opened and closed by a signal achieving perfect on–off switching for guest recognition. The next exploits metal-accumulated molecular systems bearing oligo C=N moieties as a binding site for metal ions. This strategy is remarkably useful for producing new binding sites by structural fixation of multi-metal complexes and to modulate properties of metal ions. Other cooperative molecular assembling systems for host generation are also demonstrated in this account. Metallo-frameworks and self-assembled metallo-systems recently developed in our laboratories, which have high potential for synergistic molecular functions, are discussed. Future cooperative functional systems will be widely applicable as multi-responsive multi-functional supramolecules, molecular functional cascades for successive molecular functions and function amplification. Study of cooperative and responsive molecular systems may lead to more general fields such as complex systems science, which is at the interface of chemistry, physics, biology, and mathematics.

Responsive regulation of molecular functions requires information transfer at the molecular level (Figure 1).<sup>1</sup> Receiving and releasing substances, such as molecules, metal ions, electrons, and photons, is regarded as an information transfer event. The properties of the substances, such as chirality, order, spatial arrangement, and the combination of atomic and molecular arrays can also provide information to control functions. These regulation systems are referred to as molecular systems responding to external stimuli and are also closely related to cooperative functional systems. Intramolecular and/or intermolecular interactions play a very important role in cooperative functions. In other words, intramolecular and/or intermolecular communication between different parts of the molecules is necessary to generate the observed phenomena, which are very important and interesting with respect to molecular property memory and amplification of molecular functions. Cooperative systems generally consist of two parts, a receptor site for the stimulus and an active site for the function. In biological systems, responsive and cooperative functions are essential to control enzymatic activity, transport of biologically important substances, and other functions.<sup>2</sup> These allosteric and feedback events are necessary to maintain the biological homeostasis.<sup>3</sup> Allostery is one of the most well-known and

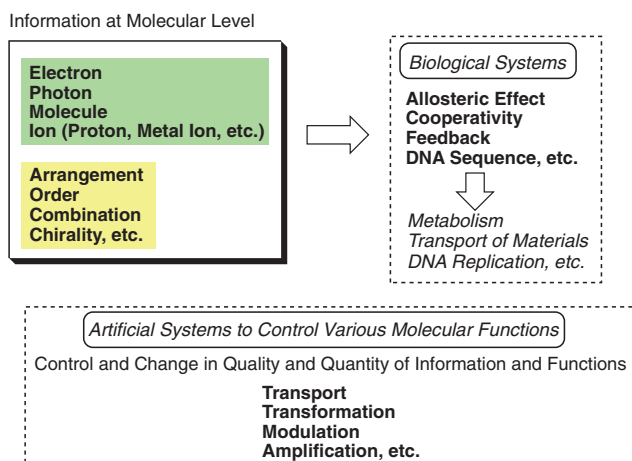


**Figure 1.** Regulation of molecular functions by utilizing molecular information.

efficient mechanisms of molecular recognition as illustrated in Figure 2. When an effector (molecule or ion), which is regarded as a first guest, binds to the allosteric host, the complexation leads to a conformational change in the host, in

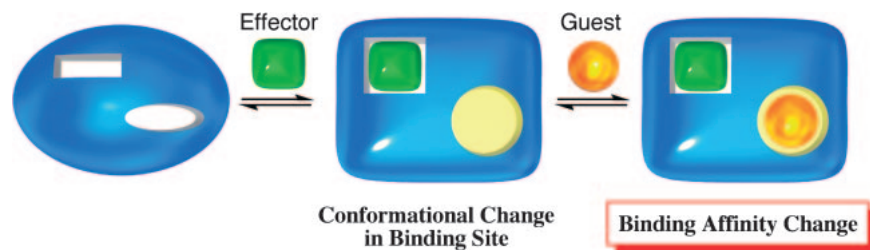


**Figure 2.** Allosteric effect on guest recognition.

particular, change to binding sites separate from the effector site. Consequently, the guest binding properties are changed by the effector. A positive allosteric effect on molecular recognition causes binding strength or selectivity to increase upon effector binding, while the negative allosterity results in a decrease of activity. Another category of allosteric effect is defined based on the types of effector and guest. When the effector and guest are the same or different, the allosteric effects are called homotropic and heterotropic, respectively.

These regulated pathways are very effective not only for dynamic control but also for fine tuning of the functions. These mechanisms can obviously be applied to artificial molecular systems with cooperative and responsive functions. In addition, supramolecular systems, whose structures are maintained by non-covalent interactions, are appropriate candidates for such sophisticated functional systems because the structures are flexible enough to change upon capturing an external signal.<sup>4</sup> Thus, we began studies of the construction of cooperative and responsive artificial supramolecular systems for molecular functional modulation.<sup>5</sup>

Based on this objective, I wish to introduce original concepts and strategies for our molecular design of cooperative systems based on the concept of information modulation at the molecular level. The first concept developed in my group is the “Pseudomacrocyclic” including pseudocrown ethers, pseudocryptands, and pseudocyclophanes as novel frameworks for responding functions by utilizing a metal ion as an effector. The second is the “Molecular Gate Responding to an External Signal.” The gate is opened and closed by a signal to achieve perfect on–off switching for guest recognition. The next idea shown here for cooperative functions is “Metal-Accumulated Molecular Systems” bearing oligo C=N moieties as a binding site for metal ions.<sup>6</sup> This strategy is remarkably useful to create a new binding site by structural fixation of a multi-metal complex and to modulate properties of the metal ions by multiple metal–metal interactions. I then demonstrate other cooperative molecular assembling systems to introduce the concept of host generation. When a first-generation host captures a guest, the host–guest complex behaves as a second-generation host, which exhibits different recognition ability. I also refer to our recent metallo-frameworks and self-assembled metallo-systems, which have high potentials for synergistic molecular functions.

### Pseudomacrocycles as Novel Frameworks for Producing Cooperative Functions

**Pseudocrown Ethers and Pseudocryptands.** At the beginning of our studies of artificial allosteric hosts, I proposed the concept of pseudomacrocycles, whose macrocyclic struc-

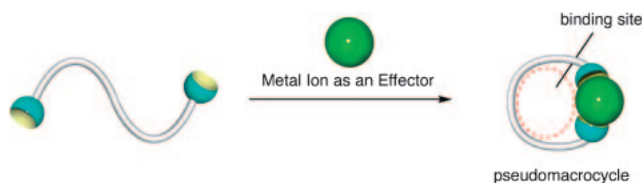


**Figure 3.** Formation of pseudomacrocyclic framework by coordination bond formation.

ture is maintained by a coordination bond instead of a covalent bond (Figure 3).<sup>5</sup> However, this idea came to me at nearly the end of my master’s program, when a professor of organic chemistry asked me why the macrocyclic structure is almost always employed for host frameworks. The simplest and most appropriate answer is probably that the macrocyclic effect can show strong and selective guest binding. But I answered that I did not think the cyclic structure is always necessary and that I was thinking about new types of linear host molecules, which can be converted to a macrocyclic host when the molecular recognition ability is needed. Although at that time this was only an idea and I did not imagine a concrete structure for the novel hosts, I believed this strategy should work to effectively control the recognition power.

Soon after I finished my postdoctoral work in the U.S., I joined Prof. Naomichi Furukawa’s laboratory at the University of Tsukuba in 1986 and started studies on the pseudomacrocycles as one of the projects that I was involved in, since Prof. Furukawa generously accepted my research plan. I chose coordination bonding to convert a linear precursor to a macrocyclic host because metal complexes generally provide various functions, which depend on the combination of the ligand and metal ions. In addition, diverse structures of the complexes are available and they are often modulated by competitive coordination to other ligands, redox reactions, and photochemical processes.

If intramolecular cyclization takes place upon the complexation of the linear host with a metal ion, a cyclic host containing the metal complex unit should be obtained. I expected this dynamic structural change would be much more effective to modulate molecular recognition than a partial conformational change of the host, which is induced by the metal binding. Because the macrocyclic effect due to reduction of the entropic loss unfavorable for the guest binding is operative, the enhancement should be enormous. One of the most famous examples of host-conformation change upon metal coordination was reported by Rebek, Jr. and co-workers (Figure 4).<sup>7</sup> A 2,2′-bipyridine moiety is incorporated into a crown ether ring. The host **1** binds to W resulting in the partial conformational change of the crown ring. The Na<sup>+</sup>/K<sup>+</sup>

selectivity in the ion transport through a liquid membrane is reversed upon the complexation.

To construct the first pseudomacrocyclic, I chose oligo-(ethylene glycol) chains as a binding site for alkali metal ions and 2,2'-bipyridine moieties as a site for transition-metal ions as an effector (Figure 5).<sup>8</sup> In the podand **2** as a precursor for the pseudocrown ether, the polyether chain is introduced into the 2,2'-bipyridine at the ortho position of the nitrogen. In addition, the bipyridines have a methyl group at the other ortho positions. I expected that the podand **2** would show a strong and selective affinity to  $\text{Cu}^{\text{I}}$  to produce a very stable tetrahedral  $\text{Cu}^{\text{I}}$  complex even under aerobic conditions because the substituents at the 6 and 6' positions are known to stabilize the geometry. In fact, the complexation took place very rapidly just by mixing **2** with  $\text{Cu}^{\text{I}}$  at room temperature to quantitatively give the red complex without the formation of any other complexes, such as oligomeric products. This excellent transformation results from the labile properties of the tetrahedral  $\text{Cu}^{\text{I}}$ -bipyridine complex. Even if the intermolecular complexation takes place, the most entropically favorable 1:1 complex is eventually produced. The lability of metal complexes is one of the most useful and important characteristics to make the desired metallo-assembly by utilizing coordination bonds. This structural change caused a dramatic enhancement of the  $\text{K}^+$  selectivity in the transport experiment across a liquid membrane. Hence,  $\text{Cu}^{\text{I}}$  acts as a metal effector for this allosteric ion recognition system.

After our work on pseudocrown ethers, other research groups reported analogous examples of pseudomacrocycles for ion recognition. For instance, the combination of oxime and phenolic hydroxy groups creates a strong coordination site for various metal ions (Figure 6).<sup>9</sup> The linear **3** reacts with  $\text{Ni}^{\text{II}}$ ,  $\text{Zn}^{\text{II}}$ , and  $\text{Cu}^{\text{II}}$  to give the corresponding metal complexes **4a** containing a  $\text{Ba}^{2+}$  ion as a template. An X-ray crystallographic

analysis of the  $\text{Zn}^{\text{II}}$  and  $\text{Cu}^{\text{II}}$  complexes clarified the heterometallic structures. Macrocyclic **5a**·Mo preferentially captures  $\text{Li}^+$  over  $\text{Na}^+$ , while the larger macrocyclic **5b**·Mo binds  $\text{Na}^+$  more strongly (Figure 7).<sup>10</sup> In the case of the Pd complex

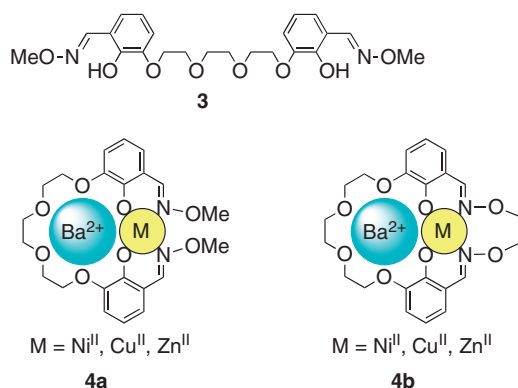


Figure 6. Dinuclear complexes of oxime-containing hosts **4**.

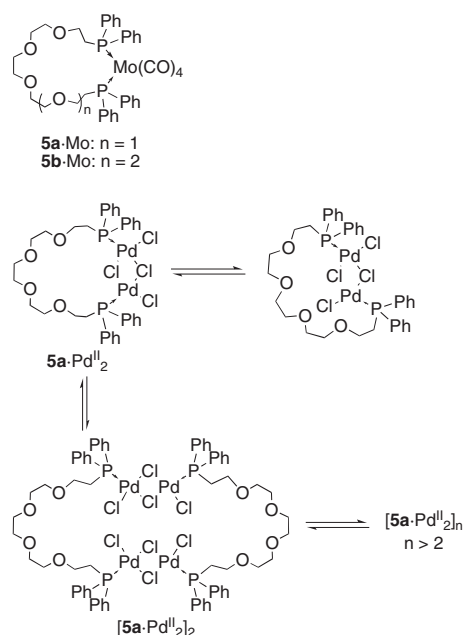


Figure 7. Pseudomacrocyclic compounds **5** with Mo or Pd.

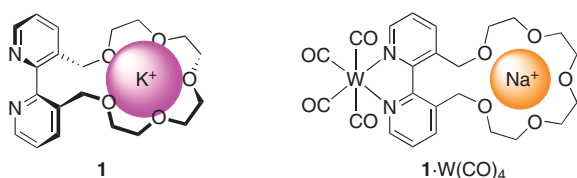


Figure 4. Host **1** and tungsten complex **1**· $\text{W}(\text{CO})_4$ .

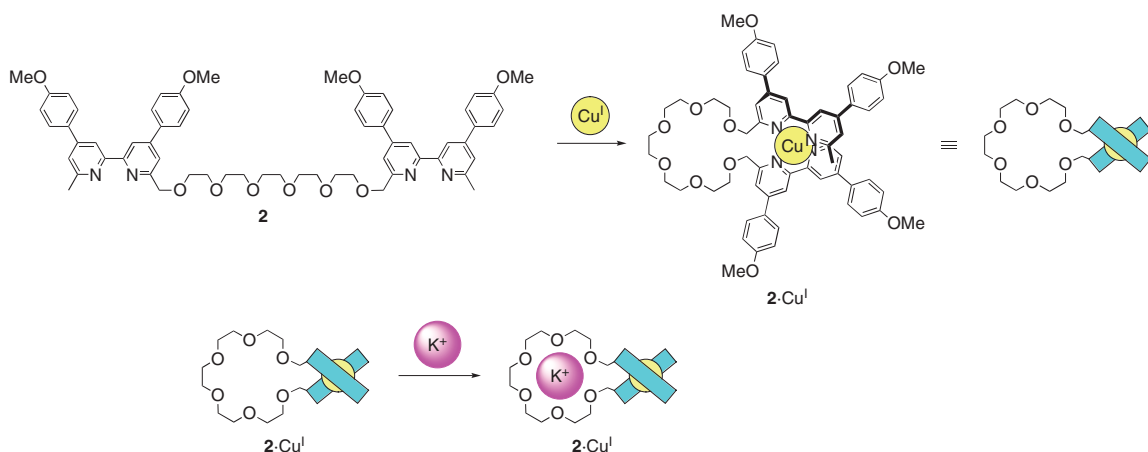
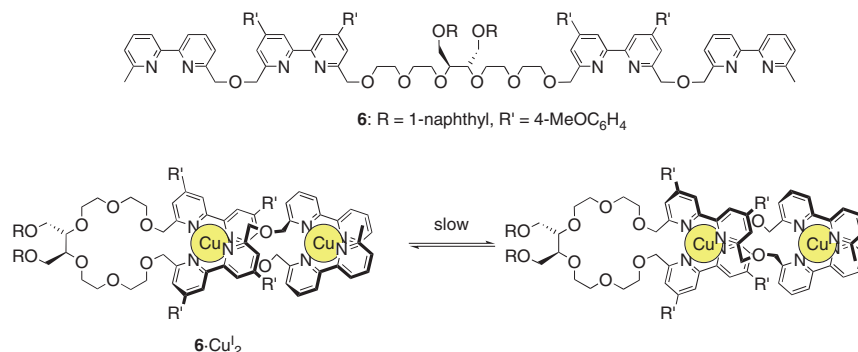


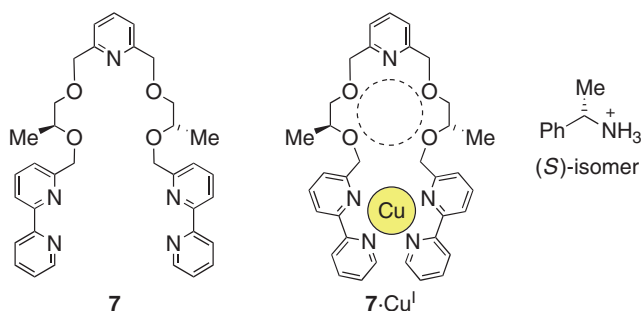
Figure 5. Formation and function of pseudocrown ether **2**· $\text{Cu}^{\text{I}}$ .

Figure 8. Chiral pseudocrown ether 6·Cu<sub>2</sub><sup>I</sup>.

5a·Pd<sup>II</sup><sub>2</sub>, the equilibrium between the anti and syn structures results in a mixture consisting of macrocyclic anti–syn isomers as well as oligomeric products.<sup>11</sup>

Pseudocrown ethers with chiral auxiliaries have also been reported. We synthesized chiral podand **6** bearing four bipyridine units (Figure 8).<sup>12</sup> The podand **6** reacts with Cu<sup>I</sup> to give a diastereomeric mixture of the 6·Cu<sub>2</sub><sup>I</sup>, which is inert on the NMR time scale due to the dual complexation with Cu<sup>I</sup>, although the usual bipyridine–Cu<sup>I</sup> complexes are labile. The pseudocrown ether 6·Cu<sub>2</sub><sup>I</sup> can be used as a chiral discriminator. The <sup>1</sup>H NMR spectra of 6·Cu<sub>2</sub><sup>I</sup> in the presence of (*R*)- and (*S*)-mandelic acid salt are different. The chiral pseudocrown ether 7·Cu<sup>I</sup>, which has a very similar framework to our original pseudocrown ethers, recognizes the (*S*)-1-phenylethylammonium salt more preferentially than the (*R*)-isomer. The precursor **7** does not show any selectivity (Figure 9).<sup>13</sup>

Chiral information is transferred using the chiral pseudocrown ether 8·Cu<sup>I</sup>, which is obtained very easily by the treatment of **8** with Cu<sup>I</sup> (Figure 10).<sup>14</sup> The 8·Cu<sup>I</sup> complex exists as a diastereomeric mixture of helical and non-helical isomers (42:58). However, we found that the addition of Na<sup>+</sup> to

Figure 9. Chiral pseudocrown ether 7·Cu<sup>I</sup>.

the mixture shifts the ratio of 89:11 due to the Na<sup>+</sup> complexation. The coordination of the polyether oxygen atoms to Na<sup>+</sup> makes the pseudomacrocyclic structure more rigid and changes the stereochemistry of the Cu–bipyridine moiety. One of the most interesting features in our system is that the chiral structure of the Cu<sup>I</sup> complex is controlled by the achiral guest Na<sup>+</sup>. Reversion of the chiral properties was also performed using electrons (redox reactions) as an achiral stimulus (Figure 11).<sup>15</sup> The CD sign of 9·Cu<sup>I</sup> is regulated by

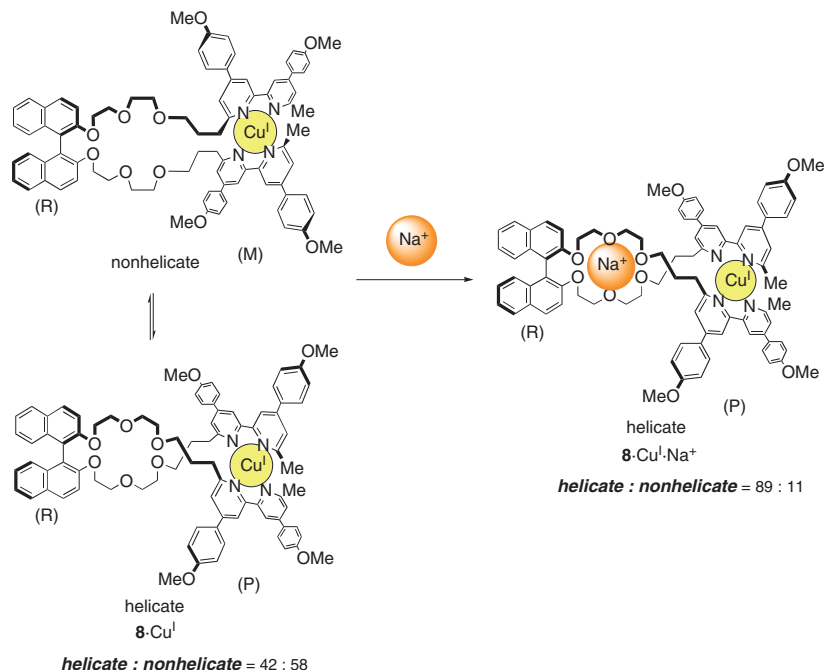


Figure 10. Modulation of chiral information by an achiral guest.

the interconversion between the  $\text{Cu}^{\text{I}}$  and  $\text{Cu}^{\text{II}}$  states. Recently, achiral anion  $\text{NO}_3^-$  was used as an external signal to change the chirality of the metal complex  $\mathbf{10} \cdot \text{Co}^{\text{II}}$  (Figure 12).<sup>16</sup>

The concept of the pseudomacrocycles can also be applied in a straightforward fashion to the synthesis of bicyclic metallohosts, i.e., pseudocryptands. We reported the first example of a pseudocryptand by using the complexation of  $\text{Cu}^{\text{I}}$  and double-armed diazacrown ether  $\mathbf{11}$  (Figure 13).<sup>17</sup> The host  $\mathbf{11} \cdot \text{Cu}^{\text{I}}$  binds to an alkali metal ion in the cavity. We synthesized a more sophisticated allosteric ionophore on the basis of the pseudocryptand framework. The designed precursor for the

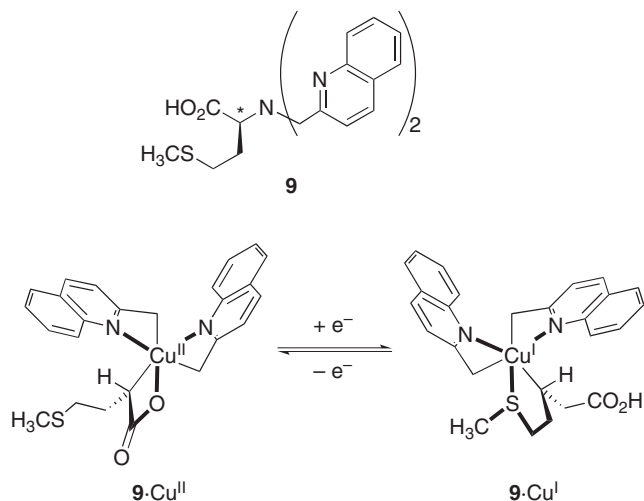


Figure 11. Modulation of chiral structure by redox reaction.

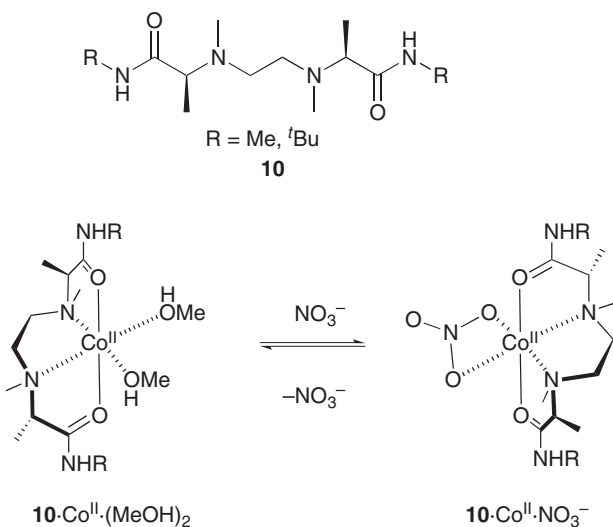


Figure 12. Modulation of chiral structure by anion.

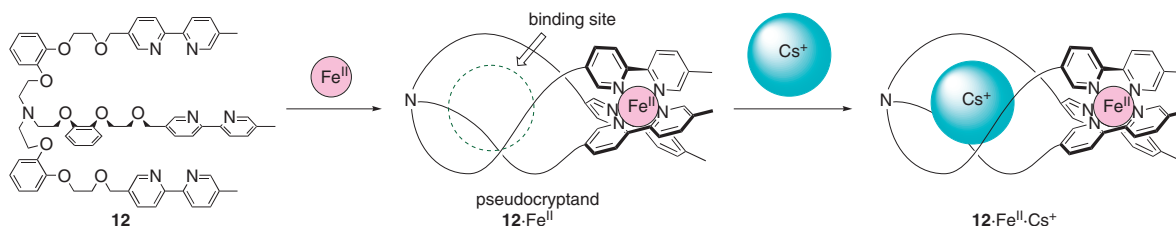


Figure 14. Formation and function of pseudocryptand  $\mathbf{12} \cdot \text{Fe}^{\text{II}}$ .

pseudocryptand is a tripodand bearing a 2,2'-bipyridine moiety at the terminal of each polyether chain (Figure 14).<sup>18</sup> The tripodand  $\mathbf{12}$  reacts very quickly with  $\text{Fe}^{\text{II}}$  to quantitatively give the corresponding 1:1 red complex  $\mathbf{12} \cdot \text{Fe}^{\text{II}}$  as a pseudocryptand. The metal-free  $\mathbf{12}$  recognizes alkali metal ions in the preferential order of  $\text{Na}^+ > \text{K}^+ > \text{Rb}^+ > \text{Cs}^+$ . In contrast, the Fe complex  $\mathbf{12} \cdot \text{Fe}^{\text{II}}$  binds to larger metal ions  $\text{Cs}^+$  ( $K_a = 4700 \text{ M}^{-1}$ ) and  $\text{Rb}^+$  ( $630 \text{ M}^{-1}$ ) much more strongly and shows no affinity to  $\text{Na}^+$ . Thus, this molecular system exhibits a very high positive allosteric effect on the  $\text{Cs}^+$  binding and a completely negative effect on the  $\text{Na}^+$  binding using the  $\text{Fe}^{\text{II}}$  ion as an effector with respect to the  $K_a$  values. In an ion transport experiment through a liquid membrane, a similar selectivity was observed. To the best of our knowledge, this is the first example of an allosteric ionophore that shows a positive and a negative allosteric effect using the same effector. An X-ray crystallographic study clearly elucidated the origin of the allostery (Figure 15). In  $\mathbf{12} \cdot \text{Fe}^{\text{II}}$ , the three polyether chains are assembled in a helical fashion to form a cavity as a binding site for the cationic guests. Noteworthy is the fact that in the  $\mathbf{12} \cdot \text{Fe}^{\text{II}} \cdot \text{Cs}^+$  complex, all the oxygen atoms coordinate to the  $\text{Cs}^+$  ion, and the  $\text{CH}-\pi$  interactions stabilize the complex. One of the methylene protons adjacent to the bipyridine skeleton locates just on the center of an electron-rich catechol moiety in another chain.  $^1\text{H}$ NMR spectral changes in the presence of  $\text{Cs}^+$  also support this geometry in solution. If the Fe complex  $\mathbf{12} \cdot \text{Fe}^{\text{II}}$  would bind to the smaller size cation  $\text{Na}^+$ , the complex must shrink to make the cation-dipole interactions favorable for the  $\text{Na}^+$  binding. This contact, however, definitely prohibits the induced-fit shrinking because this is the maximum contact of the proton with the benzene ring. It is usually very difficult to suppress the induced-fit motion of the host upon the guest binding. However, the  $\text{CH}-\pi$  contacts in our system play these two roles to increase and decrease the  $K_a$  values according to the size of the cationic guests.

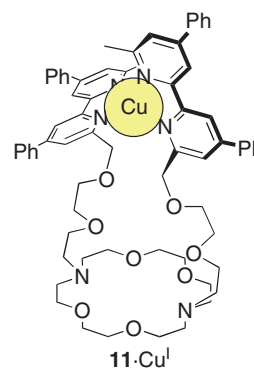


Figure 13. Pseudocryptand  $\mathbf{11} \cdot \text{Cu}^{\text{I}}$ .



Allosteric Fe binding was achieved by Shanzer et al. using compounds **13a** and **13b**, which possess amide–hydroxamic acid moieties in the chains (Figure 16).<sup>19</sup> **13a** and **13b** show a stepwise binding behavior toward  $\text{Fe}^{\text{III}}$  ions. The second Fe complexation of **13a** is weaker (negative effect) than the first Fe binding. However, **13b** instead shows a positive effect. We synthesized a protonated tricyclic pseudocryptand **14**· $\text{Fe}^{\text{II}}$ · $\text{H}^+$  bearing a triazacrown unit by the treatment of **14**,  $\text{Fe}^{\text{II}}$ , and  $\text{HBF}_4$  (Figure 17).<sup>20</sup> **14**· $\text{Fe}^{\text{II}}$ · $\text{H}^+$  shows a unique binding affinity to a cationic guest. **14**· $\text{Fe}^{\text{II}}$ · $\text{H}^+$  does not bind  $\text{Na}^+$ ,  $\text{K}^+$ ,  $\text{Rb}^+$ , and  $\text{Cs}^+$ , but interacts with  $\text{Mg}^{2+}$  and  $\text{Ca}^{2+}$  in a 1:1 manner.

A similar pseudocryptand framework, which is generated by complexation of 2,2'-bipyridine with a metal ion, was expected to be useful for the regulation of the anion recognition because the electrostatic interaction between the cationic metal center and an anionic guest should occur during the guest binding. Since the tris(2,2'-bipyridine)iron(II) complex shows reversible and stepwise redox behaviors,<sup>21</sup> the charge of the complex can be changed by suitable redox reactions. Thus, we designed podand **15** as a precursor for the  $\text{Fe}^{\text{II}}$ -pseudocryptand as an anion receptor that has a switchable anion binding ability by changing the charge of the metal center (Figure 18).<sup>22</sup> The three urea units as a hydrogen bond donor are incorporated into

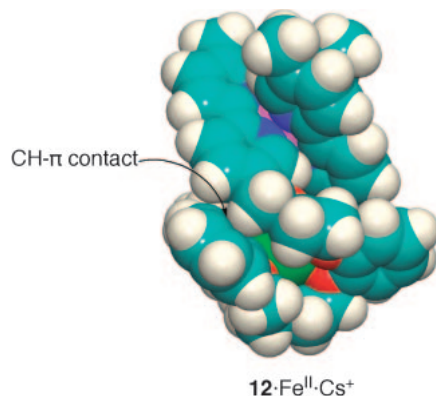


Figure 15. X-ray molecular structure of **12**· $\text{Fe}^{\text{II}}$ · $\text{Cs}^+$  with the space-filling representation.

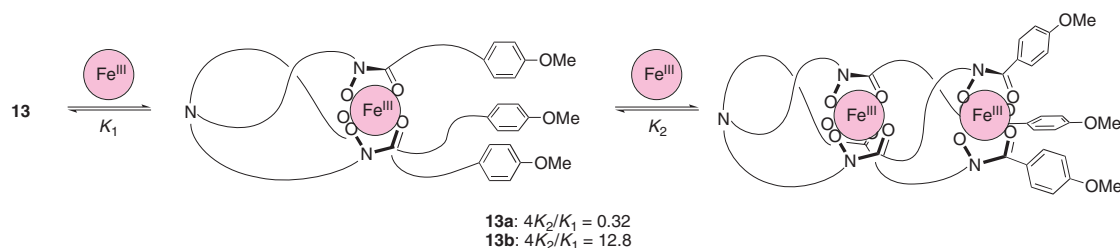
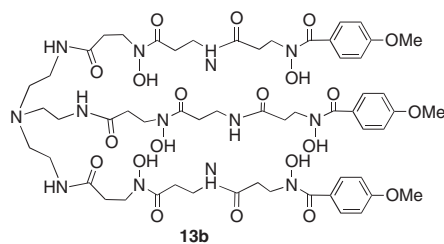
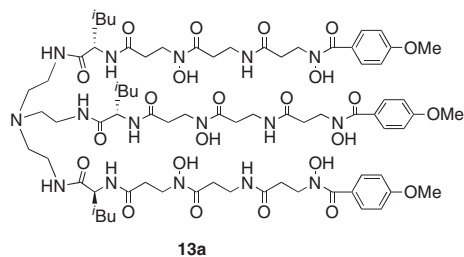


Figure 16. Allosteric complexation with  $\text{Fe}^{\text{III}}$ .

the chains bearing 2,2'-bipyridine as a binding site for  $\text{Fe}^{\text{II}}$ . If the three chains are assembled by the  $\text{Fe}^{\text{II}}$  complexation, the cavity surrounded by the chains should interact with an anionic guest through multiple hydrogen bonds and the electrostatic force with the metal center due to the close proximity. The  $^1\text{H}$  NMR and ESIMS support the fact that **15**· $\text{Fe}^{\text{II}}$  strongly and selectively binds a  $\text{Cl}^-$  anion in the cavity. As we expected, the anion affinity is stepwise and reversibly regulated by the electrochemical processes. The binding constants,  $K_a$ , were calculated from the cathodic shifts of the redox potentials. The  $K_a$  values of the more oxidized states are significantly higher than those of the less oxidized. X-ray crystallography indicates that two more interactions between the host and  $\text{Cl}^-$  contribute to the recognition (Figure 19). One is non-classical hydrogen bonding,  $\text{CH}\cdots\text{Cl}^-$ , and the other is an anion– $\pi$  interaction between  $\text{Cl}^-$  and the isocyanuric acid core. Pseudocryptands with imidazolium moieties **16**· $\text{Fe}^{\text{II}}$  were reported to be also good  $\text{Cl}^-$  binders, although the regulation of the anion binding was not examined (Figure 20).<sup>23</sup> Examples of the anion receptors described above unambiguously indicate a significant contribution of the Coulombic interactions to the anion binding. This strategy is generally employed for strong ion pair recognition.<sup>24</sup>

Multi-step regulation of the anion recognition was achieved by our calix[4]arene derivative **17** consisting of two different cation binding sites and one anion binding site (Figure 21).<sup>25</sup> The polyether moieties and ester groups create the binding site A for hard cations, and the 2,2'-bipyridine moieties (site B) can bind to a soft cation, such as  $\text{Ag}^+$ . Actually, **17** strongly captures  $\text{Na}^+$  and  $\text{Ag}^+$  in sites A and B, respectively. The

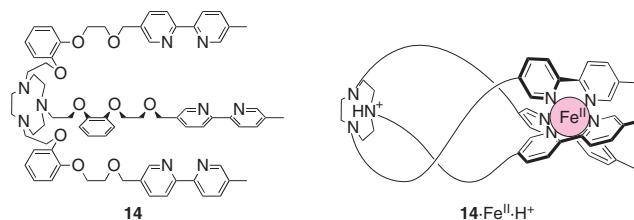
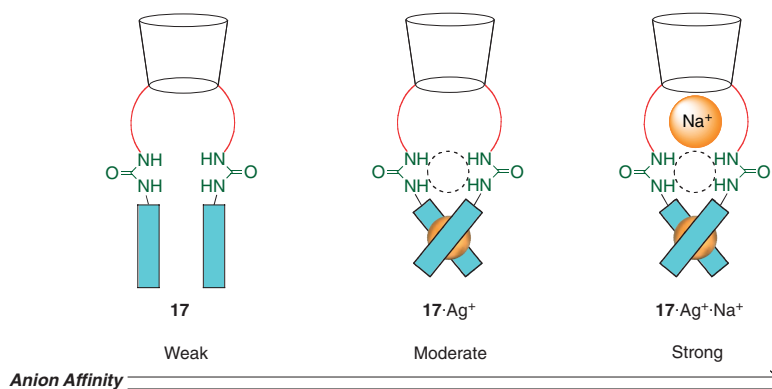
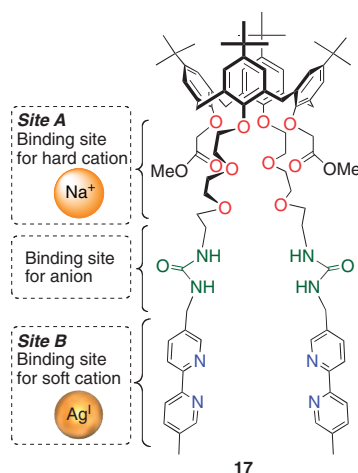
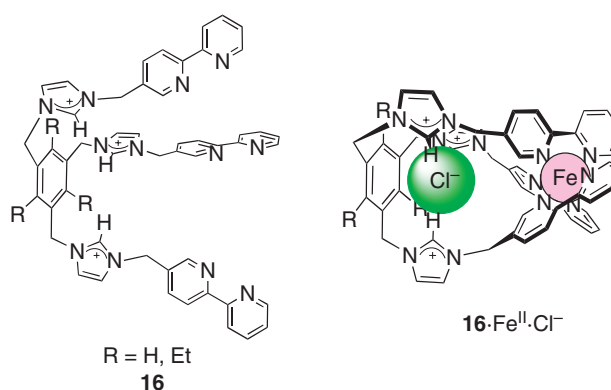
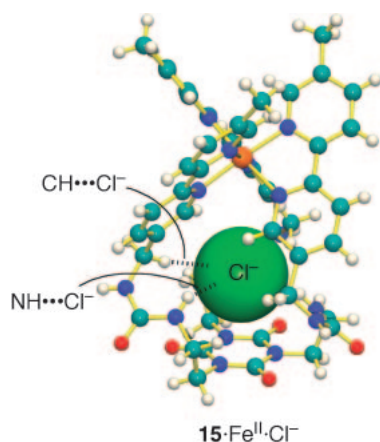
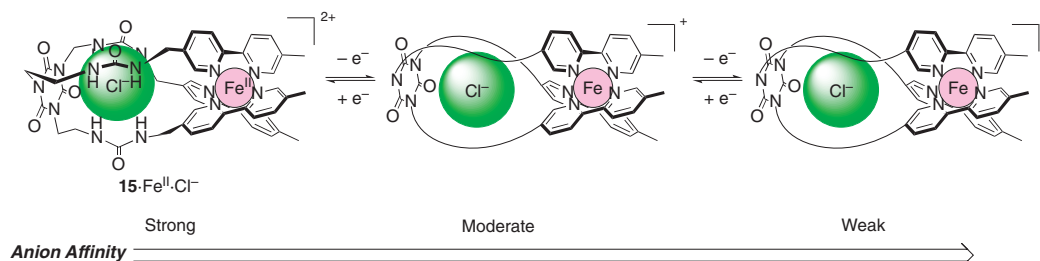
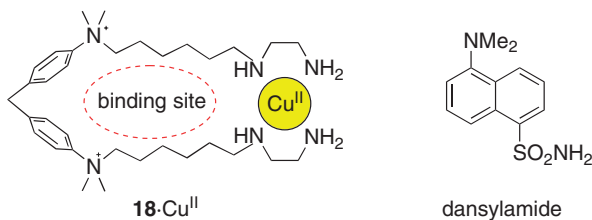
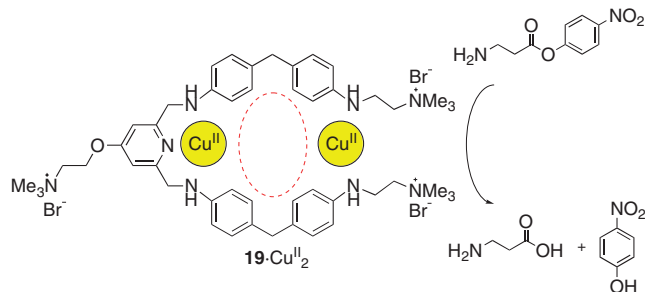


Figure 17. Pseudocryptand **14**· $\text{Fe}^{\text{II}}$ · $\text{H}^+$ .



complex  $17 \cdot \text{Ag}^+$  is regarded as a pseudocryptand. The urea functionalities provide hydrogen bond donor protons to interact with the anionic guests. Since the two cation binding sites closely locate to the anion binding site, the favorable electrostatic cation–anion interactions should effectively work. Interestingly, a dramatic enhancement of the anion recognition was observed in the presence of  $\text{Na}^+$  and  $\text{Ag}^+$ . Even anions with a very weak basicity, such as the triflate and tetrafluoroborate anions, are captured by  $17 \cdot \text{Na}^+ \cdot \text{Ag}^+$ . This binding mode is regarded as an ion-pair recognition, which has attracted much attention in supramolecular chemistry because a precise (strong and selective) recognition of the ionic guests is often performed due to the electrostatic interaction between the cation and anion coincidentally captured in the binding site.<sup>24</sup>

Multiple regulation of the guest recognition will be very useful to construct molecular sensors with a tunable sensitivity. If the sensitivity is not controllable, each molecular sensor with a highly different sensitivity is almost always designed on the basis of a different concept and design strategy. A highly sensitive sensor is not suitable for monitoring a guest at high concentrations. Of course, a sensor with a low sensitivity cannot detect a trace amount of substrate. A very large dynamic range for monitoring the guest over a wide range of concentrations is necessary, although rational molecular design seems to be very difficult. Molecular sensors, whose sensitivity responds to external stimuli, are extremely suitable to achieve a large dynamic range because only one molecular sensor can cover a wide range of concentrations without any laborious

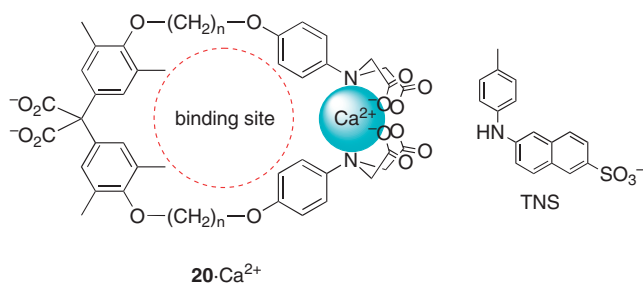
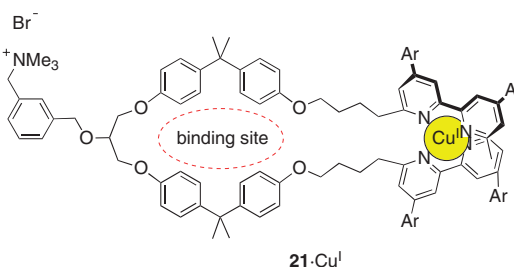
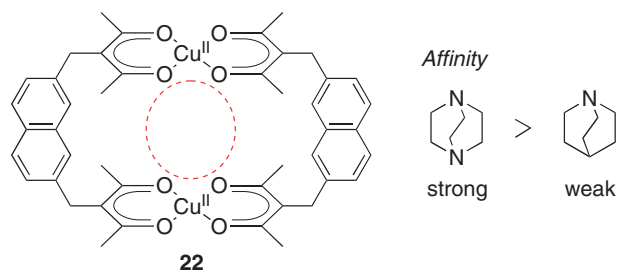
Figure 22. Pseudocyclophane  $18 \cdot \text{Cu}^{\text{II}}$ .Figure 23. Pseudocyclophane  $19 \cdot \text{Cu}^{\text{II}}_2$ .

synthesis, and the proper sensitivity can be easily selected according to the guest concentration just by adding the appropriate stimulus without any other processes, such as isolation of the sensor from the monitoring sample.

#### Pseudocyclophane and Other Related Metallo-Hosts.

Coordination bond formation can be used to form pseudocyclophanes, which may provide a binding site for organic molecules. We and other groups have developed functionalization of pseudocyclophanes. The linear diammonium molecule **18** possesses ethylenediamine moieties as a binding site for transition metals.<sup>26</sup> The water-soluble complex  $18 \cdot \text{Cu}^{\text{II}}$  shows a much higher affinity to dansylamide in water than **18** (Figure 22). The pseudocyclophane **19** captures organic guests and has a guest-selective catalytic activity (Figure 23).<sup>27</sup> The nitrophenyl esters of  $\beta$ -amino acid are hydrolyzed more rapidly than the corresponding  $\alpha$ -amino acid derivatives. The complexation of the iminodiacetic acid moieties in **20** with  $\text{Ca}^{2+}$  results in intramolecular cyclization to give the pseudocyclophane  $20 \cdot \text{Ca}^{2+}$  (Figure 24).<sup>28</sup> The 6-(*p*-toluidine)-2-naphthalene sulfonate (TNS) anion is captured in the cavity in water ( $n = 4$ ,  $K_a = 5000 \text{ M}^{-1}$ ). The hydrophobic effect obviously plays an important role in the recognition. We synthesized a functionalized pseudocyclophane  $21 \cdot \text{Cu}^{\text{I}}$ , which recognizes the flavin mononucleotide sodium salt (FMN) (Figure 25).<sup>29</sup> The efficiency for the FMN transport through a liquid membrane is greater than **21** because a multiple recognition of FMN is available in the case of  $21 \cdot \text{Cu}^{\text{I}}$ .

Multi-metal pseudomacrocycles have been reported for functional molecules. Chelate ligands have often been employed to form multi-metal pseudomacrocyclic compounds due to their strong coordination power to various metal ions. Monodentate ligands can also efficiently work to produce macrocyclic metallo-frameworks, and these studies have been well reviewed.<sup>30</sup> Thus, this section is focused on reviewing several typical examples of multi-metallic macrocycles on the basis of chelate complexation.

Figure 24. Pseudocyclophane  $20 \cdot \text{Ca}^{2+}$ .Figure 25. Pseudocyclophane  $21 \cdot \text{Cu}^{\text{I}}$ .Figure 26. Metallohost **22**.

Compound **22** is an early example of a multi-metallo host generated by the complexation of **22** and  $\text{Cu}^{\text{II}}$  in a 2:2 stoichiometry (Figure 26).<sup>31</sup> The association constant of this ditopic receptor **22** with 1,4-diazabicyclo[2.2.2]octane (dabco) is  $220 \text{ M}^{-1}$  due to the coordination of the nitrogen atoms of dabco to the  $\text{Cu}^{\text{II}}$  centers. However, the corresponding monoamine, quinuclidine, is only  $7 \text{ M}^{-1}$ . This indicates that the distance between the two  $\text{Cu}^{\text{II}}$  ions nicely fits in the position of the nitrogen atoms of the guest to increase the affinity. The phenylalanine moieties of **23** react with Co and Ni to give the metal complexes, which recognize aromatic hydrocarbon guest such as pyrene in water due to a hydrophobic effect (Figure 27).<sup>32</sup> The Ru-containing host **24** was prepared by the reaction of 3-hydroxy-2-pyridone with the  $\pi$ -arene complex (Figure 28).<sup>33</sup> The compound **24** captures  $\text{Li}^+$  or  $\text{Na}^+$  in MeOH or  $\text{CHCl}_3$ , but had no affinity to  $\text{K}^+$ . The complex **24** also behaves as a redox responsive host.  $\text{BF}_4^-$ , as an anionic template, promotes the formation of a 4:4 rectangular metallo-



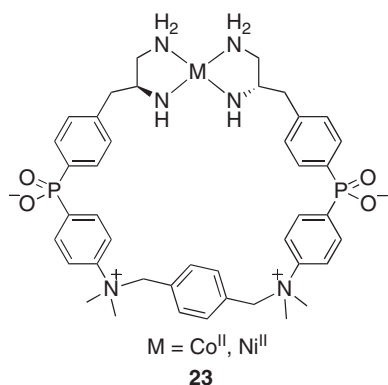


Figure 27. Metallohost 23.

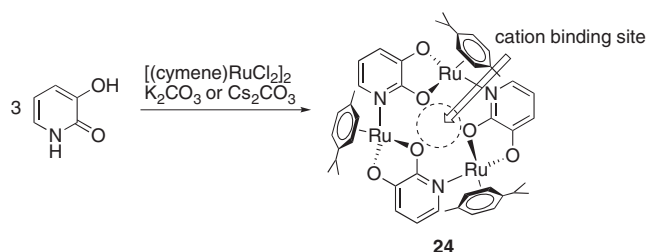
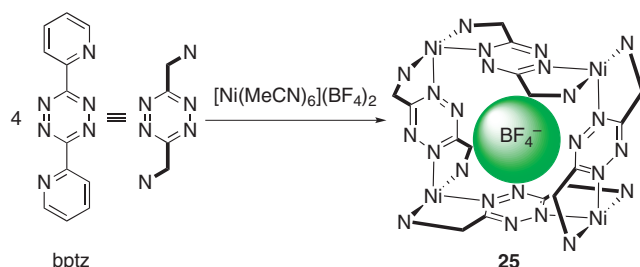


Figure 28. Metallohost 24.

Figure 29.  $\text{BF}_4^-$  complex 25.

framework **25** from  $[\text{Ni}(\text{MeCN})_6](\text{BF}_4)_2$  and bptz (Figure 29).<sup>34</sup> The pentameric complex **27** was obtained from the hydroxamic acid derivative **26** and  $\text{CuSO}_4$  in the presence of  $(\text{UO}_2)\text{SO}_4$ . An analogous cyclic chiral pentamer **29** was synthesized from **28** in a similar fashion (Figure 30).<sup>35</sup> A lanthanide ion locates in the cavity of **29**. The treatment of the diketone ligand **30** with  $\text{Fe}^{\text{III}}$  in the presence of KH as a base produces the cryptate **31** in good yield (Figure 31).<sup>36</sup> This indicates that the first complexation with  $\text{Fe}^{\text{III}}$  fixes the molecular structure favorable for the second reaction. Metal cryptates **33** are also generated from  $[\text{TiO}(\text{acac})_2]$  and the podand **32** bearing catechol moieties at the ends of the chains by template assistance of the alkali metal ions with a suitable size for the cryptand cavity (Figure 32).<sup>37</sup> The complexation of bis(8-hydroxyquinoline) ligand **34** and  $\text{Ga}^{\text{III}}$  in the presence of  $\text{K}^+$  salt yielded the cryptate **35** (Figure 33).<sup>38</sup> The dinuclear Au complex **37** is another type of metallo cryptate synthesized from bis(phosphino)phenanthroline **36** and Au in the presence of a template salt, such as  $\text{NaPF}_6$  and  $\text{TIPF}_6$  (Figure 34).<sup>39</sup>

Macrocyclic metallo-structures are sometimes dramatically changed by an additional ligand or guest. For example, weak coordination bonds between the oxygen–Rh in **38** are cleaved

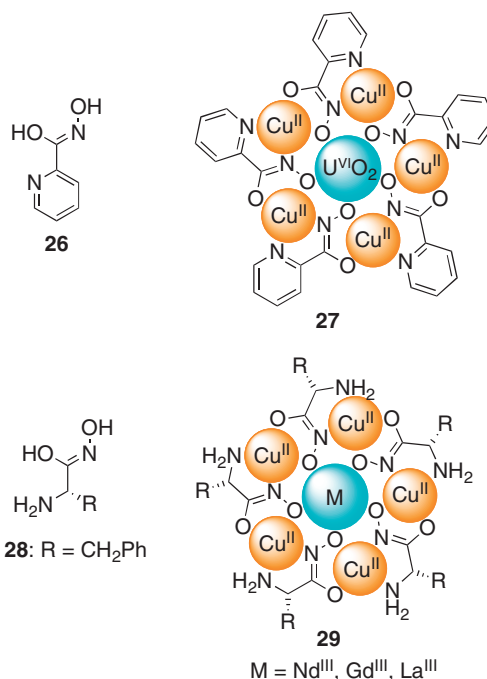


Figure 30. Multi-metallohosts 27 and 29.

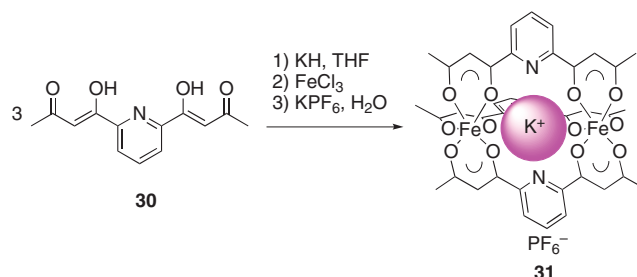


Figure 31. Formation of multi-metal complex 31.

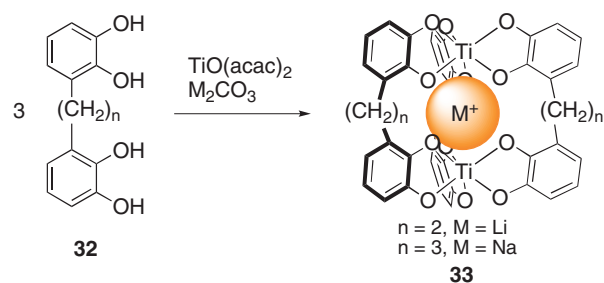


Figure 32. Formation of multi-metal complex 33.

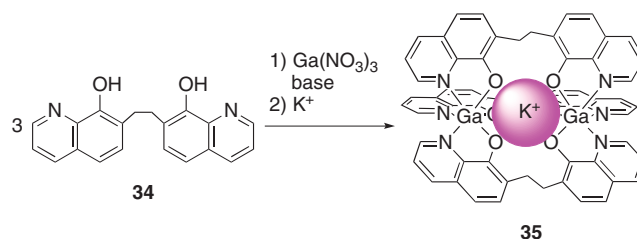


Figure 33. Formation of multi-metal complex 35.

by the addition of CO and MeCN to afford the larger-sized macrocyclic complex **39** (Figure 35).<sup>40</sup> The complex **38** reacts with 1,4-diisocyanobenzene to give the host–guest complex **40**, while the longer isocyanide 4,4'-diisocyanobiphenyl generates a molecular cylinder **41**. The host–guest interaction can drastically and efficiently change the metallo-frameworks. The dinuclear Ga<sup>III</sup> complex **42** was quantitatively converted to the tetranuclear Ga<sup>III</sup> complex **43** by the addition of tetramethylammonium chloride to stabilize the inclusion complex (Figure 36).<sup>41</sup>

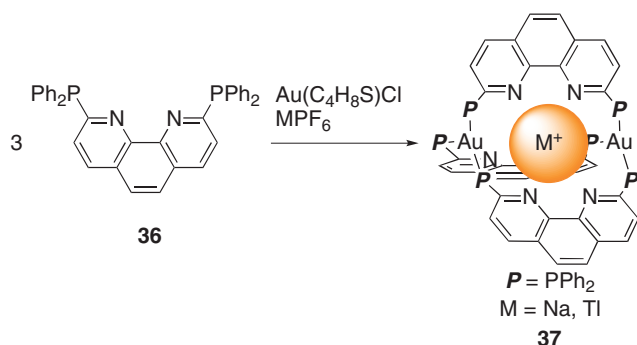


Figure 34. Formation of multi-metal complex **37**.

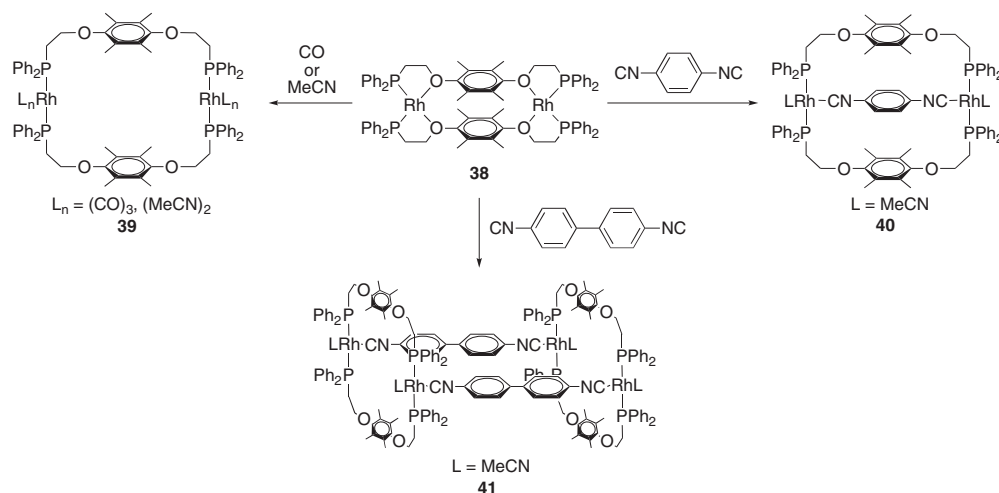


Figure 35. Structural regulation of Rh complex **38**.

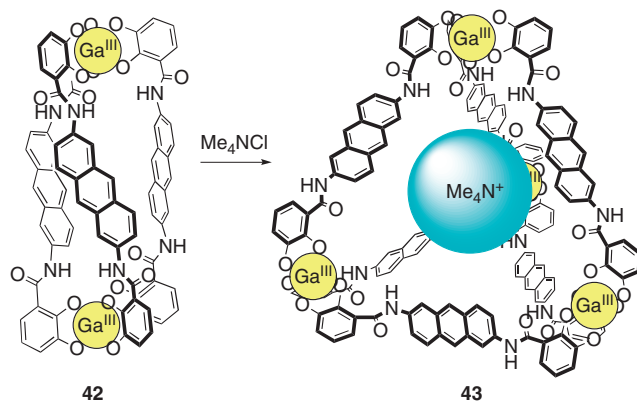


Figure 36. Structural change of metallohost **42** by cation recognition.

### Regulation of Guest Recognition by a Molecular Gate Responding to an External Stimulus

Structural changes in the hosts responding to external signals have often been employed to control their guest recognition power. Among the stimuli, redox processes effectively change the host structures. The redox interconversion between thiols and disulfides is one of the most convenient methods to control structure and functions, as seen in ribonuclease.<sup>42</sup>

The linear polyether **44<sub>red</sub>** and **45<sub>red</sub>** containing thiol functionalities are oxidized to give the corresponding macrocyclic disulfide **44<sub>ox</sub>** and **45<sub>ox</sub>** in a moderate yield, respectively (Figure 37).<sup>43</sup> Quantitative conversion from the dithiol host to the disulfide host was achieved using our biscrown ether **46** because the oligomeric by-products, which would be obtained from the intermolecular reactions, are not formed due to the proximate location of the dithiol groups of **46** (Figure 38).<sup>44</sup> The binding affinity of **47** to the ammonium guest is significantly greater than that of **46** because **47** binds the ammonium guest in a face-to-face fashion. However, the close location causes a high reactivity toward autoxidation. Under aerobic conditions, **46** is quickly oxidized to the disulfide **47**. Thus, we have to be cautious to treat the reduced form **46**. In these molecular systems, the guest binding abilities are well

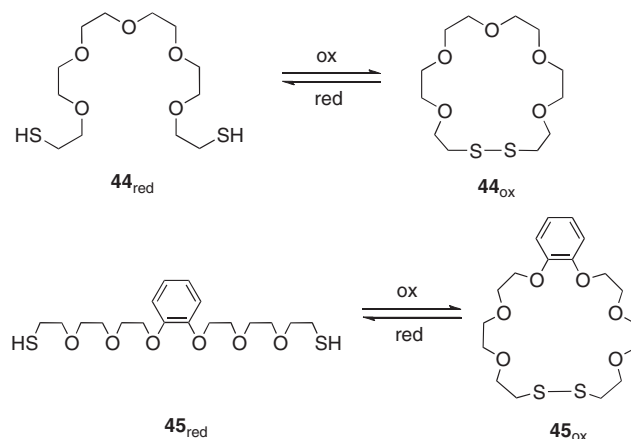


Figure 37. Redox-active crown ethers **44** and **45**.

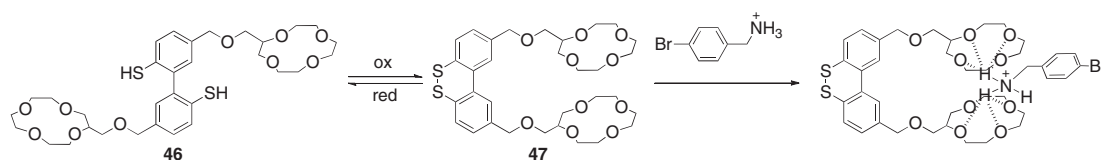


Figure 38. Quantitatively interconvertible ion recognition by redox reactions.

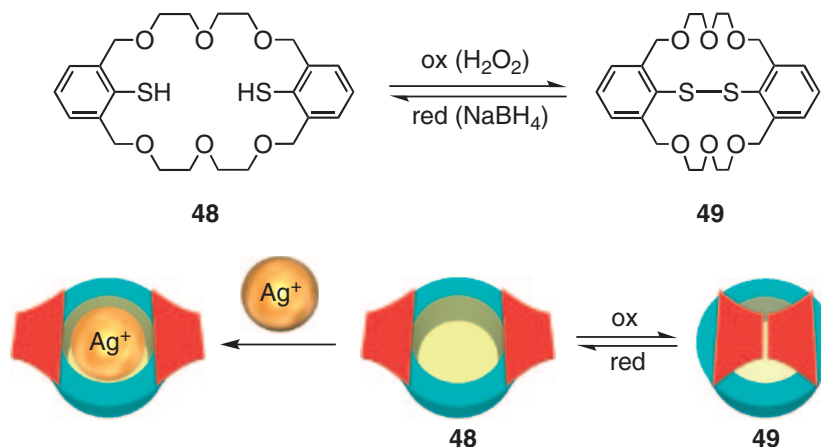


Figure 39. Redox gate for regulation of guest binding.

regulated. However, the perfect regulation of an “all-or-none switching” was not performed because both the oxidized and reduced forms have a binding site, although the binding behaviors are different. Even though the host structure is linear, the host may show a guest affinity due to the induced-fit structural change. To solve this problem, I proposed the concept of “Responding Gate in the Recognition Site.” In the inactive state of the host, the gate is closed thus prohibiting the guest binding. In contrast, the gate in the active state is open to make the binding site available. When an ideal redox gate is specifically designed for the thiol–disulfide interconversion systems, we should take the following conditions into account. (1) Quantitative interconversion between the active and inactive forms, (2) high guest selectivity of the active form, and (3) chemical and physical stability of both forms. Thus, I designed the dithiol **48** and disulfide **49** for the all-or-none switching system for ion recognition (Figure 39).<sup>45</sup> The two thiol groups locate in the host cavity and are surrounded by the polyether chains that inhibit intermolecular oxidation and autoxidation. As we expected, only the intramolecular oxidation by  $\text{H}_2\text{O}_2$  proceeded to quantitatively afford the desired disulfide **49**, while no autoxidation occurred. The disulfide perfectly reverted to the dithiol **48** by  $\text{NaBH}_4$  reduction. It is noteworthy that **48** shows a remarkably high  $\text{Ag}^+$  selectivity upon ion transport through a liquid membrane and that **49** does not have any transport ability. Interestingly, **48** was oxidized by the addition of *m*-chloroperbenzoic acid to **49** during the ion transport to cause an abrupt increase in  $\text{Ag}^+$  in the receiving phase and successive termination of the  $\text{Ag}^+$  transport. Quantitative formation of **49** clearly rationalizes this result. The  $\text{Ag}^+$  ion captured by **48** was released by closing the gate due to the oxidation and no  $\text{Ag}^+$  transport occurred due to the quantitative formation of **49**. This is the first example of a molecular system with a redox gate, which satisfies all the

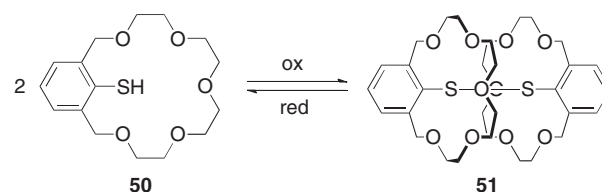


Figure 40. Intermolecularly interconvertible crown ethers **50** and **51** with different guest recognition ability.

requisites for the perfect regulation of ion recognition. Intermolecular redox reactions between the monothiol **50** and disulfide **51** can also be utilized to control  $\text{Ag}^+$  recognition (Figure 40), but the response to the oxidant is less than that of the intramolecular systems (**48** and **49**).<sup>46</sup>

Metal ions are an alternative to open and close a molecular gate. The calix[4]arene derivative **52** bearing 2,2'-bipyridine units is designed to control ion recognition by utilizing a molecular gate responding to a metal ion (Figure 41).<sup>47</sup> The host **52** binds to  $\text{K}^+$ , but this recognition is completely suppressed when  $\text{Ag}^+$  is added to **52** to form the  $\text{Ag}^+$  complex of the bipyridines. However,  $\text{Na}^+$  can again open the gate of the  $\text{52} \cdot \text{Ag}^+$  complex. This gate-assisting-regulation for guest recognition may open a new way to make novel multi-responsive function systems, which show completely different binding behaviors depending on the kinds of external stimuli.

### Multi-Metallo Molecular Systems with Cooperative Functions

Supramolecular metallo-architectures, which are prepared from several ligands and metal ions, are suitable candidates for sophisticated functions, such as cooperative molecular recognition, unique magnetic properties, selective multi-metal catalysis of chemical reactions, and novel optical properties

because the metal-to-metal interactions are expected not only to change the chemical and physical properties of the metal complexes, but also cause synergistic effects on the functions.<sup>48</sup> In addition, spatial arrangement of the metal ions incorporated into the supramolecules may create a unique space surrounded by the metal ions and ligand. Thus, this space provides novel circumstances for guests that are captured in the cavity,<sup>49</sup> because the cavity may possess a different field from the outside in terms of electrostatic, magnetic, and/or hydrophobic properties. Furthermore, the recognition ability and chemical catalysis efficiency and selectivity may significantly change when the metal ions as an interacting or a catalytic site are placed at the suitable positions. There have been many reports of multi-metal catalysis in biological and artificial systems.<sup>50</sup> Diverse applications in molecular devices and functional materials are anticipated by using multi-metal molecular systems.

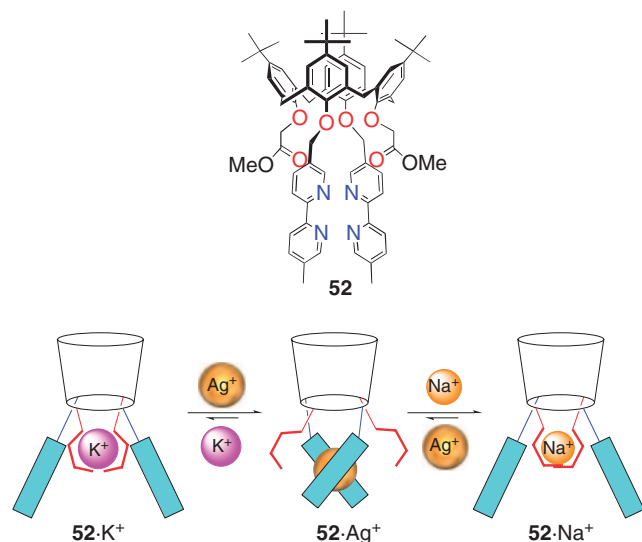


Figure 41. Molecular gate controlled by metal ions.

Therefore, to create synergistic and/or cooperative functions, I designed new strategies for multi-metallo systems in which several metal ions are accumulated in the restricted area produced by a multidentate ligand. Figure 42 shows typical molecular design (Strategy 1) of the cooperative function metallo-systems which I first proposed.

The C=N moieties attached to the catechol units are incorporated into the macrocyclic frameworks and are connected by a suitable linker, such as an alkylene, phenylene, and heteroatom-containing chain. These linkers should change the cavity size and functions, such as metal ligation. The N2O2 sites have frequently been used to make complexes with various metal ions, as seen in the salen and saloph derivatives. The obtained complexes show diverse functions for nonlinear optical properties,<sup>51</sup> magnetic materials,<sup>52</sup> catalysis of organic reactions, models of enzymatic reaction centers,<sup>53</sup> and building blocks for supramolecules with a unique topology.<sup>54</sup> The macrocyclic structure arranges the N2O2 ligation sites in a macrocyclic fashion. Consequently, the macrocyclic array of metal ions is formed upon complexation with the metal ions. One of the most interesting features of the macrocyclic N2O2 metal complex moieties is to form a macrocyclic arrangement of oxygen atoms that should be negatively charged due to the metal binding. Therefore, I predicted that the inner macrocyclic oxygen array is able to strongly recognize cationic guests like crown ether derivatives.

An alternative to the cyclic structure (Strategy 2) is also available from the complexation of a linear oligo N2O2 ligand with metal ions (Figure 43). The inner oxygen atoms are arranged in a macrocycle-like fashion to form a crown-ether-like cavity (C-shaped cavity). One more interesting and predictable structure obtained from the linear ligand is helical. When the length of the linear ligand is long enough, helical complexes would be produced upon the multi-metal complexation.

The third example (Strategy 3) of my molecular design to yield a macrocyclic metallo cavity is based on molecular

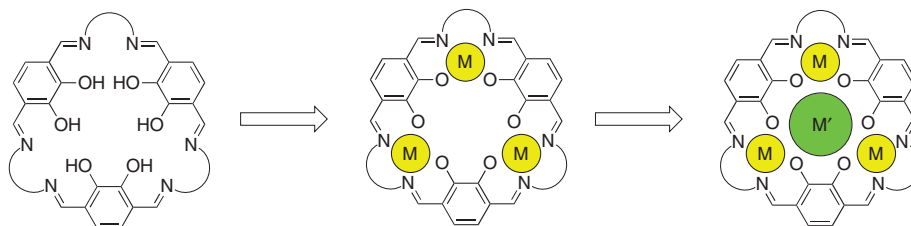


Figure 42. Strategy 1 for formation of multi-metallo systems.

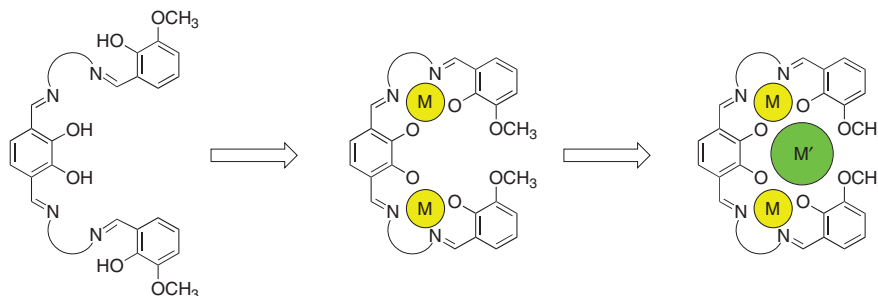


Figure 43. Strategy 2 for formation of multi-metallo systems.

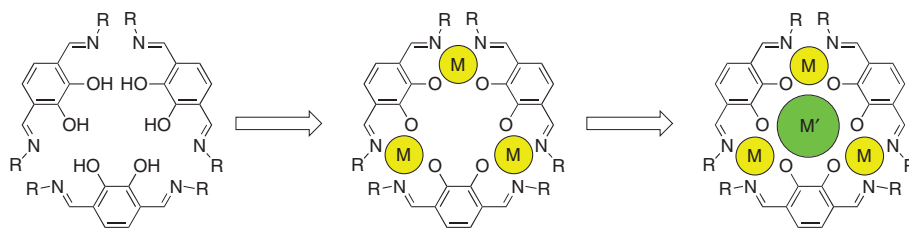


Figure 44. Strategy 3 for formation of multi-metallo systems.

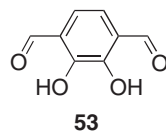


Figure 45.

assembling via coordination bond formation as shown in Figure 44, although all the ligating units are not covalently connected to each other. Coordination of the inner oxygen atoms of the macrocyclic complex to a metal ion is similarly predictable. Moreover, the template effect by the central metal ion is also expected for the preparation of the macrocyclic host, if the assembled macrocyclic structure is rigid enough. There is one more strategy that I proposed to make a macrocyclic metallo-framework (not shown). If a 1:1 mixture of the bis(salen) like unit and mono(salen) analog is treated with metal ions, a macrocyclic metallo-assembly would be afforded.

In all these basic principles, several metal ions are put into the restricted areas of the macrocyclic complexes to make metal accumulated systems, which provide novel chemical and physical properties.

When we started this research project in 1996, I was convinced that the key intermediate to synthesize these oligo *N2O2* ligands is the 1,4-diformyl-2,3-dihydroxybenzene (**53**) (Figure 45).<sup>55</sup> The simplest way to make **53** seemed to utilize the reaction of the corresponding dilithium salt with DMF, but we did not succeed in the synthesis of **53** at that time. I suspended this project for a while, but I started it again in 2000, because Dr. S. Akine joined my group as a research associate. After a careful literature survey, we synthesized **53** via the simple dilithiation of veratrole with *n*-BuLi in a reasonable yield, although this route is essentially the same as that of my first synthetic plan. As I expected in the molecular design, various compounds bearing the C=N moieties were obtained from **53** and used to develop functions of the corresponding multi-metal complexes.<sup>56</sup>

At first however, we faced a solubility problem with common organic solvents to prepare the macrocyclic compound **54**, but we definitely obtained **54** in 91% by a very slow condensation reaction (Figure 46).<sup>55a</sup> Reinhoudt and co-workers reported that the crown ether analogs **4a** and **4b**, which possess a Schiff base or an oxime moiety that provides an *N2O2* binding site to metal ions.<sup>9</sup> Stable metal complexes were synthesized in which a transition-metal ion is bound in the *N2O2* site. Since the reported results and preliminary empirical calculation suggest the oxime functionality in place of a Schiff base group may generate an effective and similar binding site,<sup>57</sup> Akine proposed the incorporation of the oxime group as a

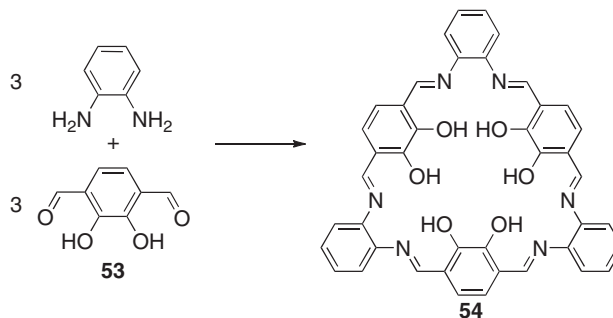


Figure 46. Formation of tri(saloph) ligand **54**.

possible linker into the original framework. After careful discussion, we started this oxime functionalization. Later we noticed that the oxime functionality is much less reactive to the disproportionation reaction than the Schiff base derivatives.<sup>58</sup> This low reactivity is very important to construct unsymmetrical supramolecular structures containing the C=N groups by avoiding the formation of undesired symmetric compounds (vide infra). Actually, the cyclic oxime analog **55** was synthesized and the solubility to the common organic solvents is sufficiently high probably due to the lower planarity of the oxime structure than the Schiff base (Figure 47).<sup>59</sup> The reaction yield is very low (15%), but a suitable multi-metal template makes the yield very high, which is discussed later. We also prepared the monomeric unit, 1,2-bis(salicylideneaminoxy)ethane (**56**, Figure 48), which we abbreviated to salamo (or H<sub>2</sub>salamo). Salamo and their derivatives show binding affinities to a variety of metal ions.<sup>60</sup>

According to the second strategy, a linear oligooxime ligand **57** was synthesized in good yields (Figure 49).<sup>61</sup> It is noted that disproportionation of the Schiff base derivatives proceeds relatively fast, while the rate for the oxime compounds is much slower.<sup>58</sup> This disproportionation is serious when preparing unsymmetrical oligo-Schiff-base ligands because the unsymmetrical compounds may produce two kinds of symmetric compounds. The salamo unit, therefore, is very useful to make complicated supramolecules containing two or more C=N groups.

The bis(salamo) **57** reacts smoothly and cooperatively with transition-metal ions. Very interestingly, the addition of Zn<sup>II</sup> to **57** was found to form the corresponding homo trinuclear Zn<sup>II</sup> complex **57**·Zn<sup>II</sup><sub>3</sub> (1:3 complex) without observation of the intermediary 1:1 and 1:2 complexes by <sup>1</sup>H NMR spectroscopy.<sup>61</sup> In the presence of 2 equiv of Zn<sup>II</sup>, two-thirds of **57** is converted to the trinuclear complex and the remaining one-third is in the reaction mixture. This fact indicates that the complexation proceeds in a highly cooperative fashion.



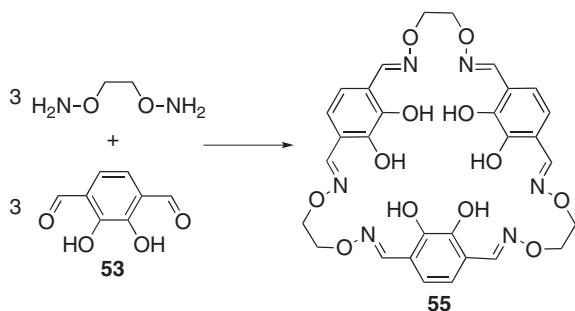
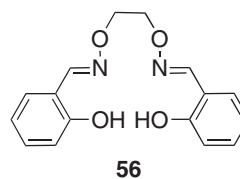
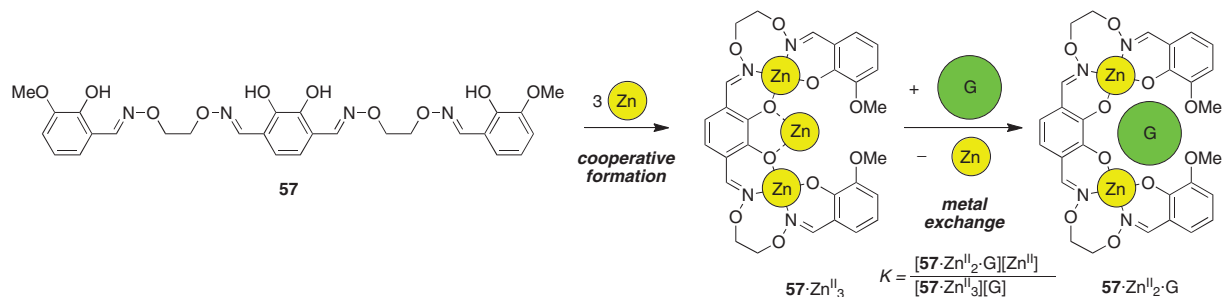
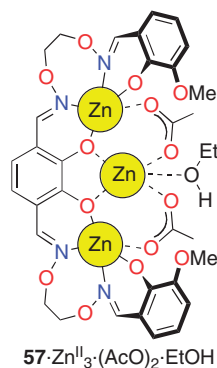
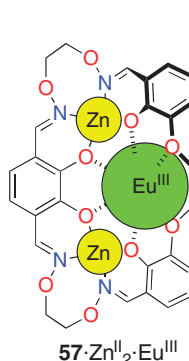
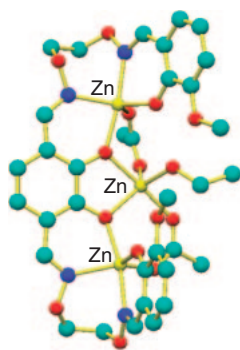
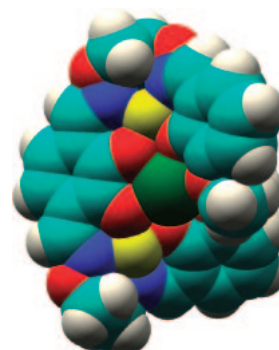
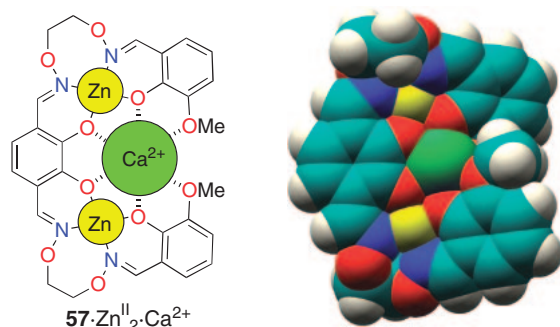
Figure 47. Formation of tri(salamo) ligand **55**.Figure 48. H<sub>2</sub>salamo.

Figure 49. Cooperative quantitative formation of homometal system and transformation to heterometal system.

Figure 50. X-ray molecular structure of **57·Zn<sup>II</sup><sub>3</sub>·(AcO)<sub>2</sub>·EtOH**.Figure 51. X-ray molecular structure of **57·Zn<sup>II</sup><sub>2</sub>·Eu<sup>III</sup>** with the space-filling representation.

The complexation of the salamo units with Zn<sup>II</sup> makes the coordinating oxygen atoms of the N2O2 sites negatively charged. Thus, the oxygen atoms should more strongly interact with the cationic guests than the neutral OH oxygens due to the electrostatic force. In addition, the C-shaped framework, which is created by the two Zn<sup>II</sup> ions in the N2O2 site, produces a relatively efficient arrangement of oxygen atoms for the central Zn<sup>II</sup> binding. X-ray crystallography revealed the characteristic coordination of acetate anions to the Zn<sup>II</sup> ions in a  $\mu_2$  fashion to stabilize the complex (Figure 50). The crystal structure also indicated that the ligation of the central Zn<sup>II</sup> is weaker than that of the other Zn<sup>II</sup> ions bound in the N2O2 sites because only two oxygen atoms of **57·Zn<sup>II</sup><sub>3</sub>** coordinate to the central Zn<sup>II</sup>. This ligation difference probably comes from the size mismatch of Zn<sup>II</sup> to the cavity. The size of the C-shaped site is too large to fit the Zn<sup>II</sup> ion. Mn<sup>II</sup>, Co<sup>II</sup>, and Ni<sup>II</sup> ions yielded similar trinuclear complexes **57·M<sub>3</sub>** (M = Mn<sup>II</sup>, Co<sup>II</sup>, and Ni<sup>II</sup>), while Cu<sup>II</sup> formed the dinuclear complex **57·Cu<sup>II</sup><sub>2</sub>** without the central metal.<sup>62</sup>

The central Zn<sup>II</sup> in **57·Zn<sup>II</sup><sub>3</sub>** should be replaced by larger metal ions such as the lanthanide ions (Figure 49). In fact, many lanthanide ions kick out the central Zn<sup>II</sup> to quantitatively afford the corresponding trinuclear heterometal complexes. Figure 51 shows the molecular structure of the **57·Zn<sup>II</sup><sub>2</sub>·Eu<sup>III</sup>** complex in a single crystal.<sup>61</sup> All the inner oxygen atoms including the methoxy oxygens coordinate to the central Eu<sup>III</sup> ion to form the helical structure. This very efficient transmetalation results from the size fitting effect and stronger electrostatic interactions between the positive charge of the trivalent europium and the negatively charged oxygen atoms. Among the alkaline earth metal ions (Mg<sup>2+</sup>, Ca<sup>2+</sup>, Sr<sup>2+</sup>, and Ba<sup>2+</sup>), the Ca<sup>2+</sup> complex is most preferentially formed because of the size fitting effect (Figure 52).<sup>63</sup> The Ca<sup>2+</sup> selectivity over Mg<sup>2+</sup> is  $>10^5$ , which was estimated from the equilibrium constant shown in Figure 49. This selectivity coefficient is comparable to those of well-known Ca<sup>2+</sup> binders, such as BAPTA and Quin 2.<sup>64</sup> However, the transmetalation did not take place at all in the case of the alkali



**Figure 52.** X-ray molecular structure of  $57 \cdot \text{Zn}^{\text{II}}_2 \cdot \text{Ca}^{2+}$  with the space-filling representation.

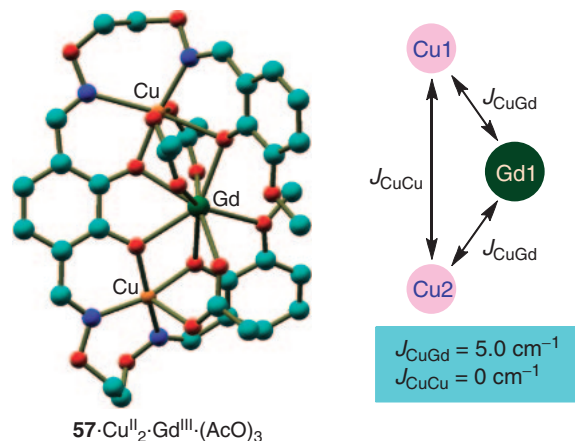


**Figure 54.** Ferromagnetic interaction in  $57 \cdot \text{Cu}^{\text{II}}_2 \cdot \text{Gd}^{\text{III}} \cdot (\text{AcO})_3$ .

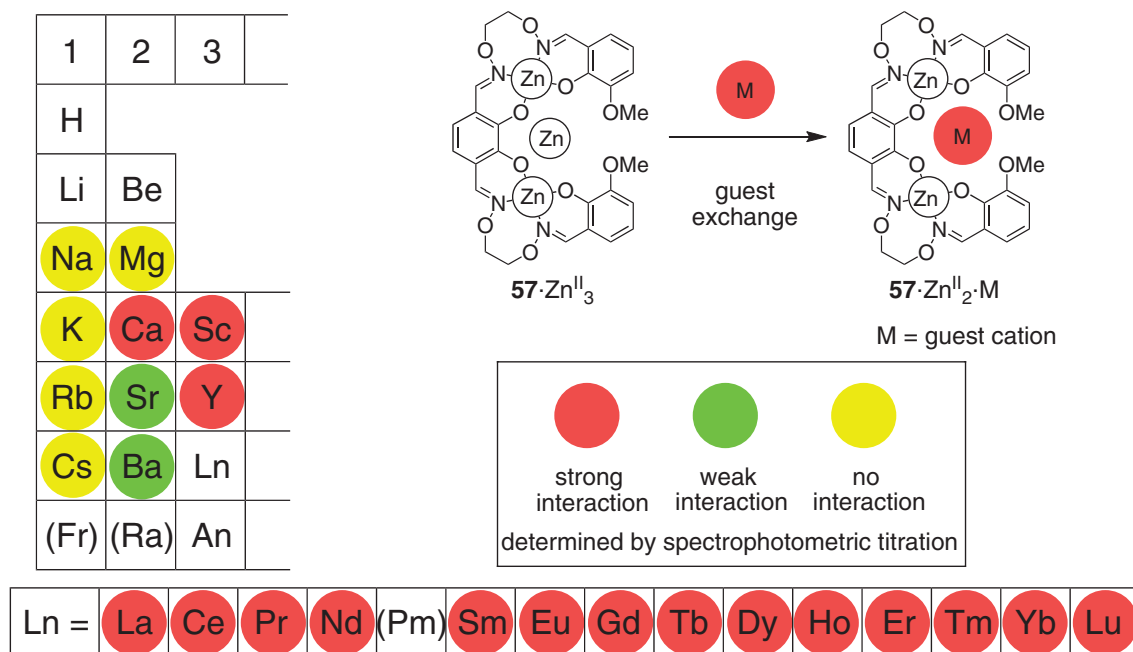


**Figure 53.** Transmetalation tendency of homo-trinuclear zinc(II) complex  $57 \cdot \text{Zn}^{\text{II}}_3$ .

metal ions. Thus, this bis(salamo) unit has the potential for application to  $\text{Ca}^{2+}$  sensing in biological tissues. The transmetalation tendency is summarized in Figure 53.<sup>55b</sup> The charge effect is primarily important, that is, the more positive metal ions tend to make the heteronuclear complex more efficient than the less positive metal ions. All the crystal structures of the lanthanide heterometal complexes were characterized by X-ray diffraction, indicating that the smaller metal ion produces a helical structure with a larger winding angle than the larger metals.

We have developed salamo derivatives for other functional systems. In the  $57 \cdot \text{Cu}^{\text{II}}_2 \cdot \text{Gd}^{\text{III}}$  complex, the ferromagnetic interaction between the  $\text{Cu}^{\text{II}}$  and  $\text{Gd}^{\text{III}}$  ions was observed at low temperature (Figure 54).<sup>65</sup> Template effects on olefin metathesis of the side chains in **58** was achieved by utilizing the bis(salamo) skeleton (Figure 55).<sup>66</sup> The macrocyclic trans isomer **59** was selectively obtained (*cis/trans* = 7:93). How-

ever, the selectivity is completely the reverse (100% *cis*) in the case of  $58 \cdot \text{Zn}^{\text{II}}_2 \cdot \text{Ca}^{2+}$ . The tris(salamo) derivative **60** reacts with  $\text{Zn}^{\text{II}}$  to afford a mixture of the complexes (Figure 56).<sup>67</sup> However, the addition of  $\text{La}^{\text{III}}$  and  $\text{Ba}^{2+}$  quantitatively converts the mixtures to the single products,  $60 \cdot \text{Zn}^{\text{II}}_3 \cdot \text{La}^{\text{III}}$  and  $60 \cdot \text{Zn}^{\text{II}}_3 \cdot \text{Ba}^{2+}$ , respectively. A guest-dependent helicity inversion rate of the complexes was observed. The  $\text{La}^{\text{III}}$  complex suffers from a slower inversion due to the stronger ligation than the  $\text{Ba}^{2+}$  complex. The salen and salamo mixed ligand bearing a chiral auxiliary at the salen moiety reacts with  $\text{Zn}^{\text{II}}$  and  $\text{La}^{\text{III}}$  to give the heterotetranuclear complex  $61 \cdot \text{Zn}^{\text{II}}_3 \cdot \text{La}^{\text{III}}$  (Figure 57).<sup>68</sup> Interestingly, the molecular structure in the solid state is absolutely left-handed and the complexes are assembled to create a superhelical structure.

Macrocyclic multi-metallo molecular systems are constructed on the basis of the first strategy using a tri(saloph) framework. The introduction of oligo(ethylene glycol) chains

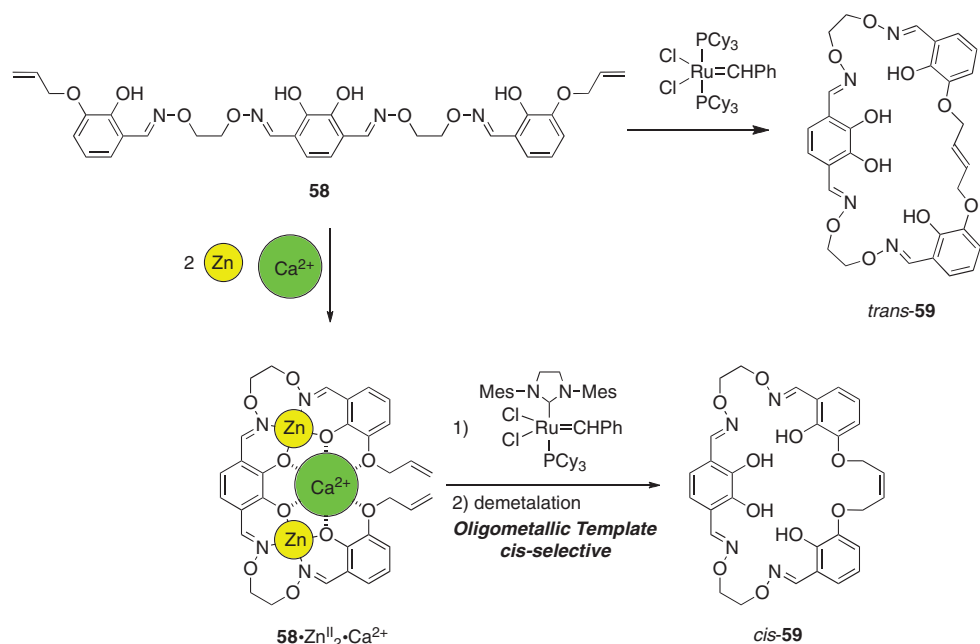
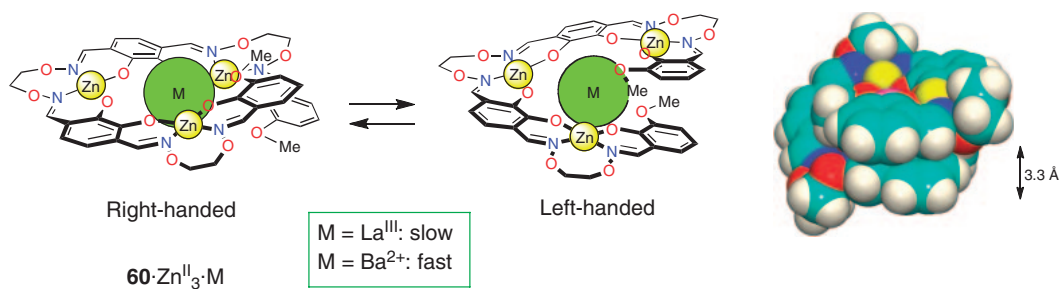
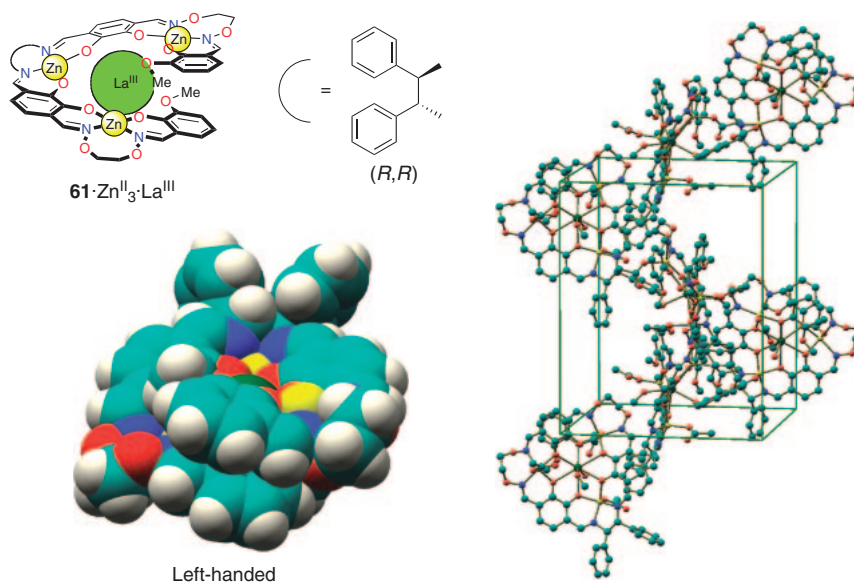
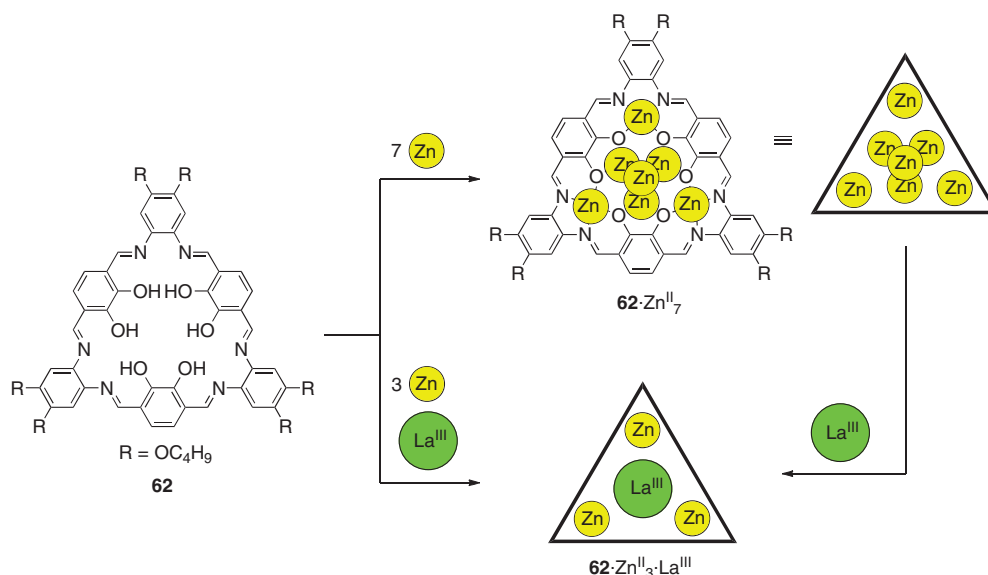


Figure 55. Olefin metathesis controlled by metalation.

Figure 56. Helicity inversion in heterometal complex **60·Zn<sup>II</sup><sub>3</sub>·M** (M = La<sup>III</sup> and Ba<sup>2+</sup>).Figure 57. Supercoiled structure of **61·Zn<sup>II</sup><sub>3</sub>·La<sup>III</sup>**.

into the skeleton makes the tri(saloph) compounds soluble in the common organic solvents.<sup>69,70</sup> One of the most unique features of **62** is that **62** reacts with Zn<sup>II</sup> to quantitatively give

the heptanuclear Zn<sup>II</sup> complex **62·Zn<sup>II</sup><sub>7</sub>**<sup>70</sup> even in the presence of an excess amount of Zn<sup>II</sup> (Figure 58). An X-ray crystallographic analysis clarified the detailed structure of this novel



**Figure 58.** Formation of multi-metal complexes  $\text{62} \cdot \text{Zn}^{II}_7$  and  $\text{62} \cdot \text{Zn}^{II}_3 \cdot \text{La}^{III}$ .

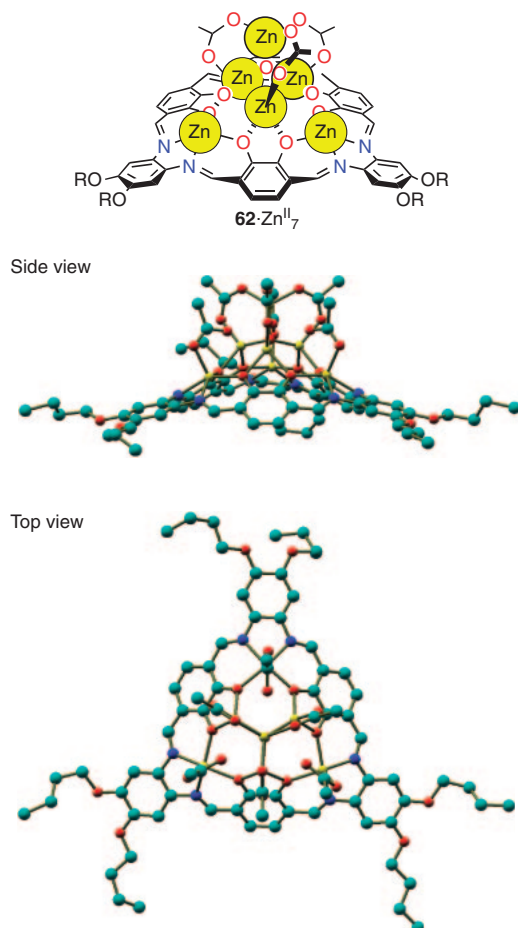


**Figure 59.** X-ray molecular structure of  $\text{62} \cdot \text{Zn}^{II}_7$ .

metal cluster complex (Figure 59). Three  $\text{Zn}^{II}$  ions sit in the  $N_2O_2$  binding sites and the catecholate moieties concomitantly coordinate to the three other  $\text{Zn}^{II}$  ions. At the center of the complex, one oxygen atom bridged the four  $\text{Zn}^{II}$  ions including the seventh  $\text{Zn}^{II}$  ion in a  $\mu_4$  fashion. This macrocyclic

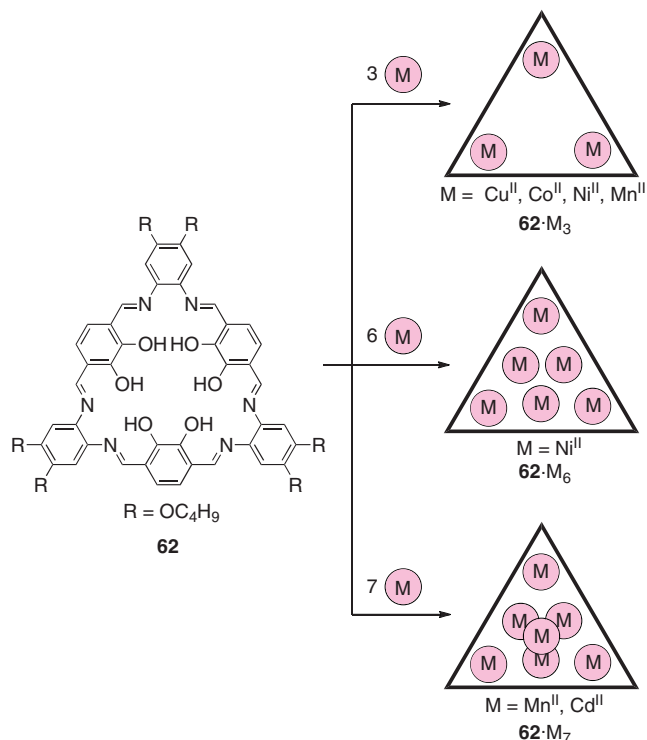
framework is believed to act as a partial template to generate the unique heptanuclear cluster because the ligand **62** provides only the base for the complexation, but does not work to wrap the entire complex as seen in usual template molecules. A similar heptanuclear complex  $\text{62} \cdot \text{Cd}^{II}_7$  was reported which further formed a capsule structure in the solid state.<sup>71</sup> The heptanuclear  $\text{Zn}^{II}$  cluster complex  $\text{62} \cdot \text{Zn}^{II}_7$  has a concave structure, but this was quantitatively transformed into the relatively planar heterotetranuclear complex  $\text{62} \cdot \text{Zn}^{II}_3 \cdot \text{La}^{III}$  just by the addition of  $\text{La}^{III}$  (Figure 58).<sup>70b</sup> Various multi-nuclear complexes of **62** with  $\text{Mn}^{II}$ ,  $\text{Co}^{II}$ , and  $\text{Cu}^{II}$  were also prepared.<sup>72</sup> A stable heptanuclear  $\text{Mn}^{II}$  complex  $\text{62} \cdot \text{Mn}^{II}_7$  was isolated in 97% yield. The trinuclear  $\text{Mn}^{II}$  and  $\text{Co}^{II}$  complexes are readily oxidized by air to the corresponding trivalent metal complexes (Figure 60). In case of  $\text{Cu}^{II}$  and  $\text{Co}^{II}$ , the trinuclear complexes were obtained even in the presence of the excess metal ions.

The homo heptanuclear complex  $\text{62} \cdot \text{Zn}^{II}_7$  was synthesized in an excellent yield from a mixture of the aldehyde **53**, diamine **63** and  $\text{Zn}^{II}$  by a one-pot reaction (Figure 61).<sup>70b</sup> In a similar manner, the hetero trinuclear complex  $\text{55} \cdot \text{Zn}^{II}_3 \cdot \text{La}^{III}$  of the salamo analog **55** was quantitatively synthesized using a  $\text{Zn}^{II}$ – $\text{La}^{III}$  multi-metal template (Figure 62). As illustrated in the third strategy, three  $\text{Zn}^{II}$  and one  $\text{La}^{III}$  ions assemble the aldehyde molecules to give the cyclic intermediary complex  $\text{53}_3 \cdot \text{Zn}^{II}_3 \cdot \text{La}^{III}$ , whose structure was ascertained by X-ray. We found that the positions of the three dialdehyde units **53** nicely fit to produce the macrocyclic structure of **55** and **62**.<sup>59</sup>

#### Our Other Approaches to Functional Molecular Systems

Compared to the covalent bond formation, molecular assembling is much more facile to produce highly functional molecules with a complex structure. One typical example is seen in protein assembling, which often gives rise to biologically important functions. Hence, this strategy has been used to make many artificial functional systems. In our first approach to the functional molecular assembly, I employed multiple hydrogen bonding to establish a new concept, the

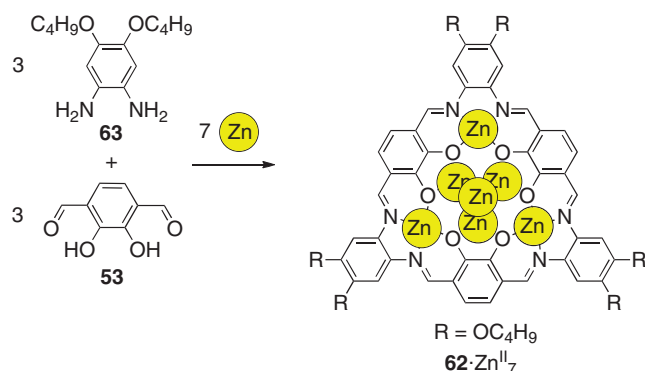
“Evolution of Host Molecules,” that is, conversion of a host as a first generation to a second generation host with a different and/or an enhanced function. This generation changing process may well continue over many generations. A flavin receptor **64** was designed as the first generation host, which has 2,6-diacylaminopyridine moieties as the binding site for flavins



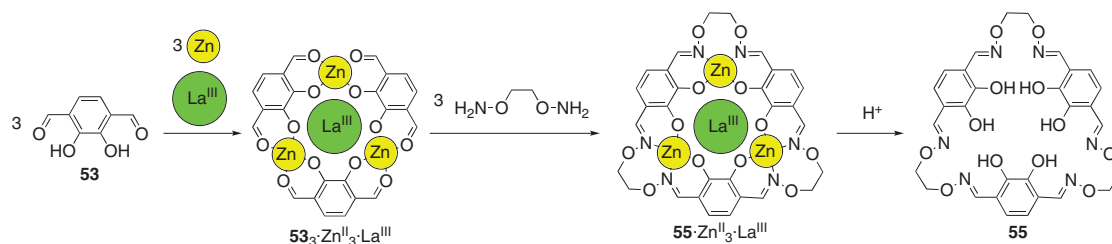
**Figure 60.** Multi-metal complexation of **62** with various metal ions.

(Figure 63).<sup>73</sup> The molecular assembly **66** as the second generation was produced from **64** and **65** through triple hydrogen bonds. The host **66** shows a higher extractability to  $K^+$  in solvent extraction because the two polyether units offered from the flavin guest **65** are concomitantly assembled to make a binding site for  $K^+$ . Another example of the functional molecular assemblies done by us is shown in Figure 64.<sup>74</sup> Host **67** (the first generation) binds to the barbituric acid derivative **68** by two triple hydrogen bonds to give the molecular assembly **69** as the second host. When the mixed solution of **67** and **68** is used as a liquid membrane, the  $Na^+$  transport efficiency is higher than that of **67** or **68** alone. This enhancement suggests that the polyether moieties of **67** and **68** are assembled to generate the stronger binding site for  $Na^+$ .

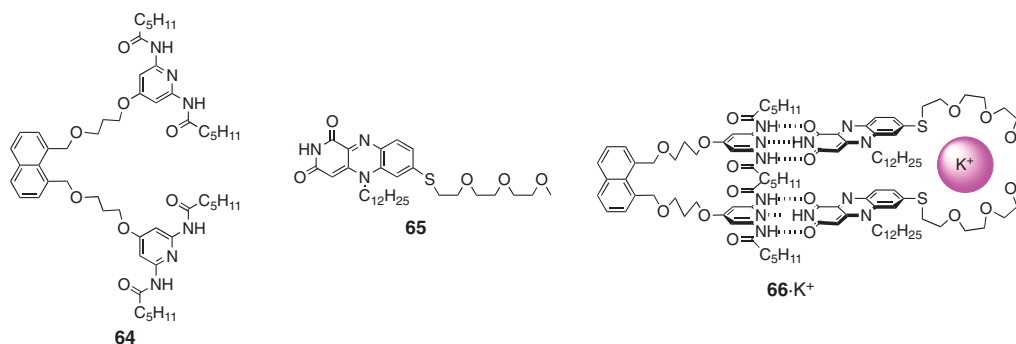
As discussed in the previous section, the *N2O2* type ligands are excellent candidates to construct molecular systems with cooperative functions. Thus, we introduced hydroxy groups into the *N2* chelate ligand, dipyrin, because the dipyrin



**Figure 61.** One-pot synthesis of heptanuclear Zn complex **62·Zn<sup>II</sup><sub>7</sub>**.

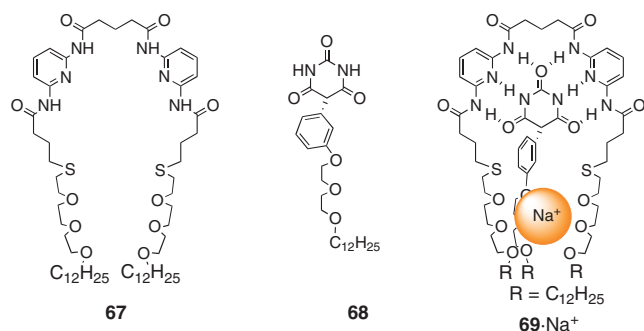
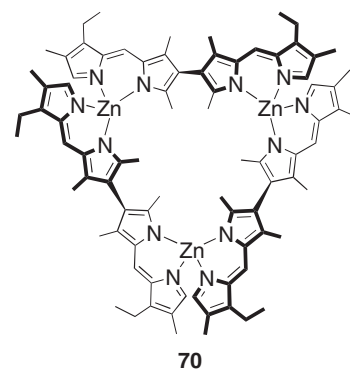
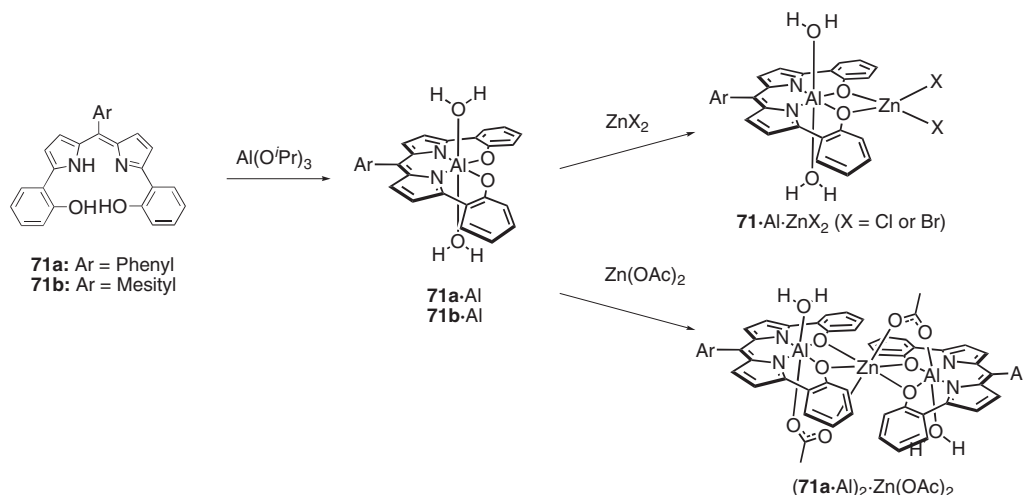


**Figure 62.** Multi-metal template synthesis of **55**.



**Figure 63.** Formation of the second generation host by utilizing molecular assembly.



Figure 64. Formulae of **67**, **68**, and **69**.Figure 65. Trimeric molecular assembly of dipyrrin derivative by complexation with Zn<sup>II</sup>.Figure 66. Synthesis of hetero-multinuclear complexes of *N2O2*-dipyrrins **71**.

derivatives and, in particular, their BF<sub>2</sub> complexes have recently attracted considerable attention due to their highly fluorescent properties. Furthermore, the *N2O2* ligand can be utilized to make molecular architectures in a molecular assembling fashion. The basic strategy for this dipyrrin project was first proposed by Dr. C. Ikeda, who joined my group as a research associate in 2005. Oligodipyrrins and bisdipyrrin derivatives were used in the early studies of supramolecular dipyrrin assemblies, although these dipyrrins are *N2* type ligands. For example, a macrocyclic metallo-trimer **70** was synthesized in high yield by the reaction of Zn<sup>II</sup> and bisdipyrrin (Figure 65).<sup>75</sup> Recently, a metal organic framework<sup>76</sup> and nanoscale aggregate<sup>77</sup> have been synthesized by complexation of the *N2* dipyrrin with a metal ion. The *N2O2* dipyrrins would then provide versatile characteristics and functions. However, only a few examples of the transition-metal complexes had been reported so far.<sup>78</sup> As seen in the salamo and saloph ligands, the metal complexes of the *N2O2* ligands would serve as a chelating moiety to other metal ions. Therefore, we prepared the Al complexes of **71a·Al** and **71b·Al** (Figure 66).<sup>79</sup> The Al complexes should have an octahedral geometry because the *N2O2* sites are suitable as a planar equatorial unit of the octahedral complex. The oxygen atoms of the *N2O2* dipyrrin–Al complex should create a stronger chelating site to the metal ion than the corresponding

boron complexes because of the lower electronegativity of Al than B. In fact, the Al complex **71a·Al** reacts with Zn(OAc)<sub>2</sub> to give the 2:1 complex (**71a·Al**)<sub>2</sub>·Zn(OAc)<sub>2</sub>. The acetate anions bridge the Al and Zn ion to stabilize the octahedral complex. In contrast, the reaction of **71·Al** with ZnCl<sub>2</sub> or ZnBr<sub>2</sub> resulted in the 1:1 complexes. The two  $\mu$ -phenoxo oxygen atoms in **71b·Al·ZnCl<sub>2</sub>**<sup>5c</sup> and (**71a·Al**)<sub>2</sub>·Zn(OAc)<sub>2</sub> coordinate to the Zn<sup>II</sup> ions (Figure 67). When **71a·Al** and **71b·Al** are converted to the **71·Al·ZnCl<sub>2</sub>** complexes, the fluorescence quantum yields significantly increase from 0.23 and 0.72 to 0.55 and 0.83, respectively.

The dipyrrin **72** has a catechol substituent at the meso position (Figure 68).<sup>80</sup> The heteroleptic complexation of **72** with BCl<sub>3</sub> gave a mixture of self-assembled supramolecules, i.e., the trimer **73a**, tetramer **73b**, and pentamer **73c**. These macrocyclic structures are maintained by the B–N and B–O bonds in a head-to-tail fashion (Figure 69). The **73a** recognizes alkali metal ions in the cavity consisting of the catecholate oxygen atoms and the electron-rich pyrrole rings. The binding constant for Cs<sup>+</sup> ( $\geq 5.5 \times 10^6 \text{ M}^{-1}$ ) is much higher than those for K<sup>+</sup> ( $1.5 \times 10^4 \text{ M}^{-1}$ ) and Rb<sup>+</sup> ( $5.7 \times 10^4 \text{ M}^{-1}$ ).

The macrocyclic dipyrrin trimer **74** and tetramer **75** were synthesized by the acid-catalyzed condensation of the bispyrrolylbenzene derivative and benzaldehyde (Figure 70).<sup>81</sup> The dipyrrin units of **74** and **75** are connected by the 2,3-

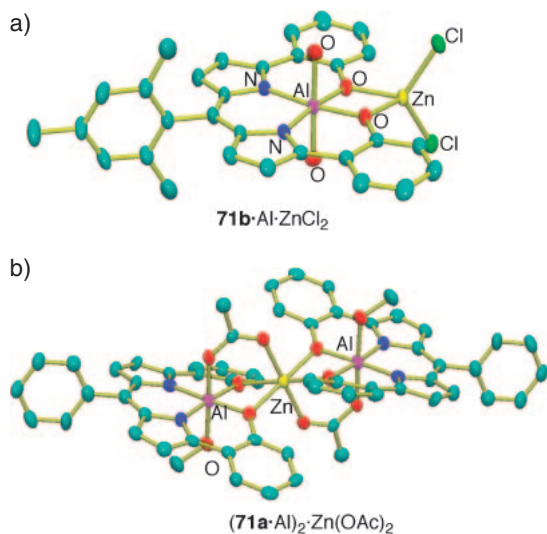


**Figure 67.** X-ray molecular structure of a)  $71b \cdot Al \cdot ZnCl_2$  and b)  $(71a \cdot Al)_2 \cdot Zn(OAc)_2$ .

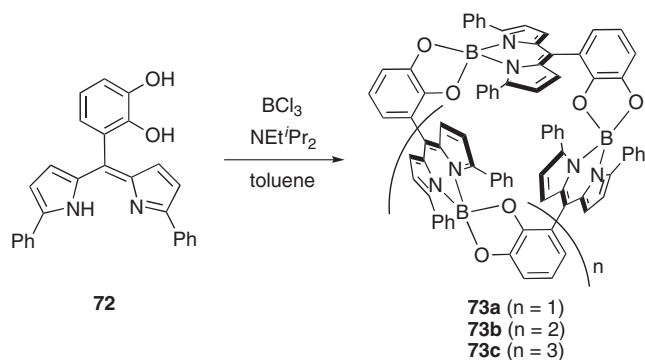


**Figure 68.** Synthetic scheme of self-assembled cyclic boron-dipyrrin oligomers **73**.

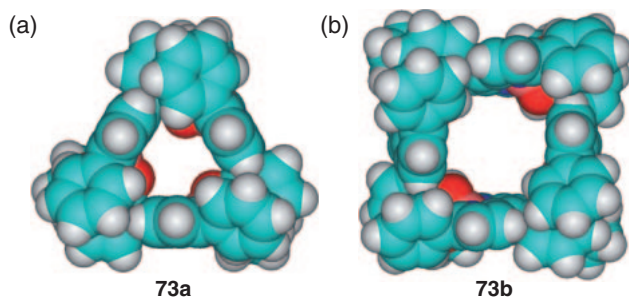


**Figure 69.** X-ray molecular structure of **73a** and **73b** with the space-filling representation.

dimethoxy-1,4-phenylene linker. In the crystalline state, **74** adopts a planar triangular structure. A spectroscopic study suggested that the conjugation along the macrocycle **74** is changed by the recognition of alkali metal ions in the cavity. The addition of  $K^+$ ,  $Rb^+$ , and  $Cs^+$  caused large bathochromic shifts of 50–60 nm, indicative of elongation of the  $\pi$ -conjugation. Based on a spectrophotometric titration, the trimer **74** was found to bind  $K^+$ ,  $Rb^+$ , and  $Cs^+$  with the association constants of  $2.1 \times 10^6$ ,  $2.3 \times 10^6$ , and  $2.5 \times 10^6 M^{-1}$ , respectively. The Hartree–Fock calculation suggests that the alkali

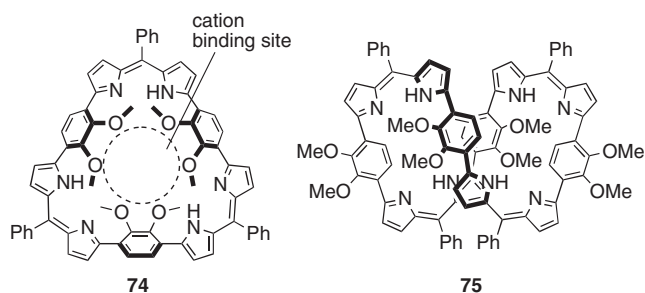


**Figure 70.** Macrocyclic dipyrins, trimer **74** and tetramer **75**.

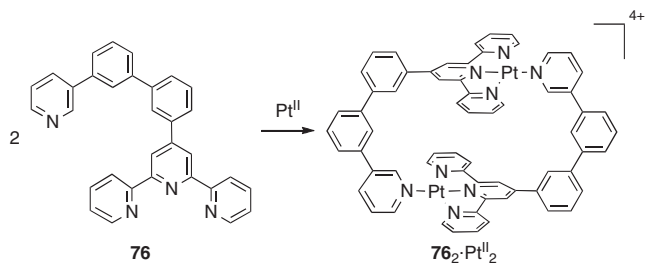


**Figure 71.** Synthesis of molecular box **762·Pt<sup>II</sup><sub>2</sub>** by coordination bond formation.

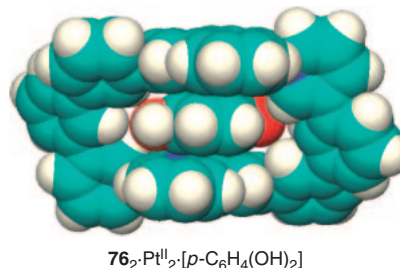


**Figure 72.** X-ray molecular structure of host-guest complex of **762·Pt<sup>II</sup><sub>2</sub>** and hydroquinone with the space-filling representation.

metal ions in the cavity are coordinated by the methoxy oxygen atoms through dipole–ion interactions. All the methoxy groups face to the inside to make the cyclic oxygen array suitable for the cation binding. On the other hand, the tetramer **75** has a twisted figure-eight structure in the solid state.

We have recently designed and synthesized an unsymmetrical ligand **76**, in which pyridine and terpyridine moieties are linked by a biphenylene spacer (Figure 71).<sup>82</sup> A molecular box **762·Pt<sup>II</sup><sub>2</sub>** was quantitatively obtained from **76** and  $Pt^{II}$ . The dimer **762·Pt<sup>II</sup><sub>2</sub>** shows an affinity toward benzene diol guests with preference in the order of para > meta > ortho. The recognition is performed by the combined contribution of the macrocyclic preorganization effect, induced-fit complexation mechanism, and electrostatic interactions including  $\pi$ – $\pi$  stacking and  $CH \cdots O$  non-classical hydrogen bonding (Figure 72).

We believe that multi-metal hosts prepared from unsymmetrical ligands and/or by heteroleptic complexation with metal ions are more useful as host frameworks suitable for the precise recognition of guests with a rather complex structure than the highly symmetric metallo-hosts.

### Conclusions and Perspectives

The transfer and modulation of the molecular information are necessary processes for cooperative molecular functions. Changes in the structure and/or the chemical and physical properties of the functional molecules always concomitantly occur along with receiving molecular information. When the functional molecules respond to external (intermolecular) as well as internal (intramolecular) stimuli, the molecules exhibit cooperative functions in principle. Along this strategic line, we have developed the pseudomacrocyclic, responsive molecular gate, a multi-metal accumulated molecular system, and molecular assembly with cooperative functions. All these molecular systems work very efficiently to change their intrinsic functions and properties by using stimuli at the molecular level. Studies of cooperative molecular systems may lead to more general fields such as complex systems science, which is at the interface of chemistry, physics, biology, and mathematics.

Future stages of cooperative functional systems will be fascinating, versatile and widely applicable. For example, molecules which respond to different stimuli in a different fashion should be very useful for preparing molecular devices with multi-functions that can be controlled by independent stimuli. One more interesting and important future objective of cooperative systems is to create molecular functional cascades that show successive molecular functions and function amplification. A similar cascading enhancement of functions is observed in the actions of medicines in biological systems. Molecular systems with responsive multi-functions will also miniaturize functional materials and open a novel way to develop molecular electronics and molecular machinery with a variety of controllable functions.

I thank all the co-workers including staff, postdocs, and students for their significant and valuable collaboration at the University of Tsukuba and Gunma University. In particular, I express my gratitude to Drs. S. Akine, T. Saiki, and C. Ikeda for their extraordinary contribution especially to the multi-metallo accumulated systems, responsive metallo gate, and dipyrin assemblies, respectively. I am indebted to Dr. M. Yamamura for his assistance in preparing the figures. I also acknowledge the financial support from the Ministry of Education, Culture, Sports, Science and Technology, Japan.

### References

- 1 a) J.-M. Lehn, *Angew. Chem., Int. Ed. Engl.* **1990**, 29, 1304. b) F. Stoddart, *Chem. Br.* **1991**, 714.
- 2 a) B. Alberts, D. Bray, J. Lewis, M. Raff, K. Roberts, J. D. Watson, *Molecular Biology of the Cell*, Garland Publishing, New York, **1983**, Chap. 13. b) L. Stryer, *Biochemistry*, 3rd ed., Freeman, New York, **1988**, Parts II and III. c) C. R. Cantor, P. R. Schimmel, *Biophysical Chemistry*, W. H. Freeman and Company, New York, **1980**, Part 3, pp. 849–1371.
- 3 a) M. F. Perutz, *Mechanisms of Cooperativity and Allosteric Regulation in Proteins*, Cambridge University Press, Cambridge, England, **1989**. b) J. Rebek, Jr., *Acc. Chem. Res.* **1984**, 17, 258. c) I. Tabushi, *Pure Appl. Chem.* **1988**, 60, 581.
- 4 a) J.-M. Lehn, *Supramolecular Chemistry*, VHC, Weinheim, **1995**. b) F. Vögtle, *Supramolecular Chemistry*, Wiley, New York, **1991**.
- 5 a) T. Nabeshima, *Coord. Chem. Rev.* **1996**, 148, 151. b) T. Nabeshima, S. Akine, T. Saiki, *Rev. Heteroat. Chem.* **2000**, 22, 219. c) T. Nabeshima, S. Akine, in *Redox Systems Under Nano-Space Control*, ed. by T. Hirao, Springer, Berlin, **2006**, Chap. 10, pp. 167–178. d) T. Nabeshima, S. Akine, *Chem. Rec.* **2008**, 8, 240. e) T. Nabeshima, S. Akine, C. Ikeda, M. Yamamura, *Chem. Lett.* **2010**, 39, 10.
- 6 S. Akine, T. Nabeshima, *Dalton Trans.* **2009**, 10395.
- 7 J. Rebek, Jr., J. E. Trend, R. V. Wattlely, S. Chakravorti, *J. Am. Chem. Soc.* **1979**, 101, 4333.
- 8 a) T. Nabeshima, T. Inaba, N. Furukawa, *Tetrahedron Lett.* **1987**, 28, 6211. b) T. Nabeshima, T. Inaba, N. Furukawa, T. Hosoya, Y. Yano, *Inorg. Chem.* **1993**, 32, 1407.
- 9 a) F. C. J. M. van Veggel, S. Harkema, M. Bos, W. Verboom, G. K. Woolthuis, D. N. Reinhoudt, *J. Org. Chem.* **1989**, 54, 2351. b) F. C. J. M. van Veggel, W. Verboom, D. N. Reinhoudt, *Chem. Rev.* **1994**, 94, 279.
- 10 A. Varshney, G. M. Gray, *Inorg. Chem.* **1991**, 30, 1748.
- 11 D. C. Smith, Jr., C. H. Lake, G. M. Gray, *Chem. Commun.* **1998**, 2771; D. C. Smith, Jr., G. M. Gray, *Inorg. Chem.* **1998**, 37, 1791.
- 12 T. Nabeshima, T. Hosoya, Y. Yano, *Synlett* **1998**, 265.
- 13 Y. Habata, J. S. Bradshaw, X. X. Zhang, R. M. Izatt, *J. Am. Chem. Soc.* **1997**, 119, 7145.
- 14 T. Nabeshima, A. Hashiguchi, T. Saiki, S. Akine, *Angew. Chem., Int. Ed.* **2002**, 41, 481.
- 15 S. Zahn, J. W. Canary, *Science* **2000**, 288, 1404.
- 16 H. Miyake, K. Yoshida, H. Sugimoto, H. Tsukube, *J. Am. Chem. Soc.* **2004**, 126, 6524.
- 17 T. Nabeshima, T. Inaba, T. Sagae, N. Furukawa, *Tetrahedron Lett.* **1990**, 31, 3919.
- 18 T. Nabeshima, Y. Yoshihira, T. Saiki, S. Akine, E. Horn, *J. Am. Chem. Soc.* **2003**, 125, 28.
- 19 S. Blanc, P. Yakirevitch, E. Leize, M. Meyer, J. Libman, A. Van Dorsselaer, A.-M. Albrecht-Gary, A. Shanzer, *J. Am. Chem. Soc.* **1997**, 119, 4934.
- 20 T. Nabeshima, Y. Tanaka, T. Saiki, S. Akine, C. Ikeda, S. Sato, *Tetrahedron Lett.* **2006**, 47, 3541.
- 21 a) Y. Kaizu, T. Yazaki, Y. Torii, H. Kobayashi, *Bull. Chem. Soc. Jpn.* **1970**, 43, 2068. b) P. S. Braterman, J.-I. Song, R. D. Peacock, *Inorg. Chem.* **1992**, 31, 555. c) B. R. Serr, K. A. Andersen, C. M. Elliott, O. P. Anderson, *Inorg. Chem.* **1988**, 27, 4499. d) S. Ferrere, C. M. Elliott, *Inorg. Chem.* **1995**, 34, 5818.
- 22 T. Nabeshima, S. Masubuchi, N. Taguchi, S. Akine, T. Saiki, S. Sato, *Tetrahedron Lett.* **2007**, 48, 1595.
- 23 a) V. Amendola, M. Boiocchi, B. Colasson, L. Fabbri, M.-J. R. Dutton, F. Ugozzoli, *Angew. Chem., Int. Ed.* **2006**, 45, 6920. b) K. Sato, Y. Sadamitsu, S. Arai, T. Yamagishi, *Tetrahedron Lett.* **2007**, 48, 1493.
- 24 a) H. Tsukube, *Tetrahedron Lett.* **1981**, 22, 3981. b) M. T. Reetz, C. M. Niemeyer, K. Harms, *Angew. Chem., Int. Ed. Engl.* **1991**, 30, 1474. c) E. A. Arafa, K. I. Kinnear, J. C. Lockhart, *J. Chem. Soc., Chem. Commun.* **1992**, 61. d) T. Nagasaki, H. Fujishima, M. Takeuchi, S. Shinkai, *J. Chem. Soc., Perkin Trans. 1* **1995**, 1883. e) P. D. Beer, S. W. Dent, *Chem. Commun.* **1998**, 825. f) M. J. Deetz, M. Shang, B. D. Smith, *J. Am. Chem. Soc.* **2000**, 122, 6201.
- 25 T. Nabeshima, T. Saiki, J. Iwabuchi, S. Akine, *J. Am. Chem. Soc.* **2005**, 127, 5507.
- 26 H.-J. Schneider, D. Ruf, *Angew. Chem., Int. Ed. Engl.* **1990**, 29, 1159.

- 27 P. Scrimin, P. Tecilla, U. Tonellato, N. Vignaga, *J. Chem. Soc., Chem. Commun.* **1991**, 449.
- 28 K. L. Cole, M. A. Farran, K. Deshayes, *Tetrahedron Lett.* **1992**, 33, 599.
- 29 T. Nabeshima, A. Hashiguchi, S. Yazawa, T. Haruyama, Y. Yano, *J. Org. Chem.* **1998**, 63, 2788.
- 30 M. Fujita, *Chem. Soc. Rev.* **1998**, 27, 417.
- 31 A. W. Maverick, S. C. Buckingham, Q. Yao, J. R. Bradbury, G. G. Stanley, *J. Am. Chem. Soc.* **1986**, 108, 7430.
- 32 F. Wang, A. W. Schwabacher, *J. Org. Chem.* **1999**, 64, 8922.
- 33 a) H. Piotrowski, K. Polborn, G. Hilt, K. Severin, *J. Am. Chem. Soc.* **2001**, 123, 2699. b) H. Piotrowski, G. Hilt, A. Schulz, P. Mayer, K. Polborn, K. Severin, *Chem.—Eur. J.* **2001**, 7, 3196.
- 34 C. S. Campos-Fernández, R. Clérac, K. R. Dunbar, *Angew. Chem., Int. Ed.* **1999**, 38, 3477.
- 35 a) A. J. Stemmler, A. Barwinski, M. J. Baldwin, V. Young, V. L. Pecoraro, *J. Am. Chem. Soc.* **1996**, 118, 11962. b) A. D. Cutland, J. A. Halfen, J. W. Kampf, V. L. Pecoraro, *J. Am. Chem. Soc.* **2001**, 123, 6211.
- 36 R. W. Saalfrank, A. Dresel, V. Seitz, S. Trummer, F. Hampel, M. Teichert, D. Stalke, C. Stadler, J. Daub, V. Schünemann, A. X. Trautwein, *Chem.—Eur. J.* **1997**, 3, 2058.
- 37 M. Albrecht, H. Röttele, P. Burger, *Chem.—Eur. J.* **1996**, 2, 1264.
- 38 M. Albrecht, O. Blau, *Chem. Commun.* **1997**, 345.
- 39 V. J. Catalano, B. L. Bennett, H. M. Kar, B. C. Noll, *J. Am. Chem. Soc.* **1999**, 121, 10235.
- 40 a) J. R. Farrell, C. A. Mirkin, L. M. Liable-Sands, A. L. Rheingold, *J. Am. Chem. Soc.* **1998**, 120, 11834. b) B. J. Holliday, J. R. Farrell, C. A. Mirkin, K.-C. Lam, A. L. Rheingold, *J. Am. Chem. Soc.* **1999**, 121, 6316.
- 41 C. Brückner, R. E. Powers, K. N. Raymond, *Angew. Chem., Int. Ed.* **1998**, 37, 1588.
- 42 C. B. Anfinsen, E. Haber, M. Sela, F. H. White, Jr., *Proc. Natl. Acad. Sci. U.S.A.* **1961**, 47, 1309.
- 43 a) M. Raban, J. Greenblatt, F. Kandil, *J. Chem. Soc., Chem. Commun.* **1983**, 1409. b) S. Shinkai, K. Inuzuka, O. Manabe, *Chem. Lett.* **1983**, 747. c) S. Shinkai, K. Inuzuka, O. Miyazaki, O. Manabe, *J. Am. Chem. Soc.* **1985**, 107, 3950.
- 44 T. Nabeshima, A. Sakiyama, A. Yagyu, N. Furukawa, *Tetrahedron Lett.* **1989**, 30, 5287.
- 45 T. Nabeshima, H. Furusawa, Y. Yano, *Angew. Chem., Int. Ed. Engl.* **1994**, 33, 1750.
- 46 T. Nabeshima, H. Furusawa, N. Tsukada, T. Shinnai, T. Haruyama, Y. Yano, *Heterocycles* **1995**, 41, 655.
- 47 T. Nabeshima, T. Saiki, K. Sumitomo, *Org. Lett.* **2002**, 4, 3207.
- 48 a) G. Schmid, *Nanoparticles: From Theory to Application*, Wiley, Weinheim, **2004**. b) H. S. Nalwa, *Encyclopedia of Nanoscience and Nanotechnology*, American Scientific, Stevenson Ranch, California, CA, USA, **2004**.
- 49 a) P. D. Beer, *Chem. Commun.* **1996**, 689. b) P. D. Beer, *Acc. Chem. Res.* **1998**, 31, 71. c) L. Fabbrizzi, M. Licchelli, G. Rabaioli, A. Taglietti, *Coord. Chem. Rev.* **2000**, 205, 85. d) A. Robertson, S. Shinkai, *Coord. Chem. Rev.* **2000**, 205, 157. e) M. H. Keefe, K. D. Benkstein, J. T. Hupp, *Coord. Chem. Rev.* **2000**, 205, 201. f) C. W. Rogers, M. O. Wolf, *Coord. Chem. Rev.* **2002**, 233–234, 341. g) P. D. Beer, J. Cadman, *Coord. Chem. Rev.* **2000**, 205, 131. h) P. D. Beer, E. J. Hayes, *Coord. Chem. Rev.* **2003**, 240, 167.
- 50 a) E. N. Jacobsen, in *Catalytic Asymmetric Synthesis*, ed. by I. Ojima, VCH, New York, **1993**. b) T. Katsuki, *Coord. Chem. Rev.* **1995**, 140, 189. c) E. N. Jacobsen, *Acc. Chem. Res.* **2000**, 33, 421.
- 51 a) S. Di Bella, I. Fragalà, *Synth. Met.* **2000**, 115, 191. b) P. G. Lacroix, *Eur. J. Inorg. Chem.* **2001**, 339.
- 52 a) T.-T. Tsou, M. Loots, J. Halpern, *J. Am. Chem. Soc.* **1982**, 104, 623. b) M. F. Summers, L. G. Marzilli, N. Bresciani-Pahor, L. Randaccio, *J. Am. Chem. Soc.* **1984**, 106, 4478.
- 53 a) J.-P. Costes, F. Dahan, A. Dupuis, J.-P. Laurent, *Inorg. Chem.* **1996**, 35, 2400. b) J.-P. Costes, F. Dahan, A. Dupuis, J.-P. Laurent, *Inorg. Chem.* **1997**, 36, 3429. c) J.-P. Costes, F. Dahan, A. Dupuis, J.-P. Laurent, *Inorg. Chem.* **1997**, 36, 4284. d) J.-P. Costes, F. Dahan, A. Dupuis, J.-P. Laurent, *New J. Chem.* **1998**, 22, 1525. e) J.-P. Costes, F. Dahan, A. Dupuis, J.-P. Laurent, *Chem.—Eur. J.* **1998**, 4, 1616. f) J.-P. Costes, F. Dahan, A. Dupuis, *Inorg. Chem.* **2000**, 39, 165. g) J.-P. Costes, F. Dahan, B. Donnadieu, J. Garcia-Tojal, J.-P. Laurent, *Eur. J. Inorg. Chem.* **2001**, 363. h) J.-P. Costes, J. M. Clemente-Juan, F. Dahan, F. Dumestre, J.-P. Tuchagues, *Inorg. Chem.* **2002**, 41, 2886. i) R. Gheorghe, M. Andruh, J.-P. Costes, B. Donnadieu, *Chem. Commun.* **2003**, 2778. j) R. Koner, H.-H. Lin, H.-H. Wei, S. Mohanta, *Inorg. Chem.* **2005**, 44, 3524.
- 54 a) G. A. Morris, S. T. Nguyen, J. T. Hupp, *J. Mol. Catal. A: Chem.* **2001**, 174, 15. b) K. E. Splan, A. M. Massari, G. A. Morris, S.-S. Sun, E. Reina, S. T. Nguyen, J. T. Hupp, *Eur. J. Inorg. Chem.* **2003**, 2348. c) S.-S. Sun, C. L. Stern, S. T. Nguyen, J. T. Hupp, *J. Am. Chem. Soc.* **2004**, 126, 6314. d) S.-H. Cho, T. Gadzikwa, M. Afshari, S. T. Nguyen, J. T. Hupp, *Eur. J. Inorg. Chem.* **2007**, 4863. e) N. C. Gianneschi, P. A. Bertin, S. T. Nguyen, C. A. Mirkin, L. N. Zakharov, A. L. Rheingold, *J. Am. Chem. Soc.* **2003**, 125, 10508. f) N. C. Gianneschi, S.-H. Cho, S. T. Nguyen, C. A. Mirkin, *Angew. Chem., Int. Ed.* **2004**, 43, 5503. g) N. C. Gianneschi, S. T. Nguyen, C. A. Mirkin, *J. Am. Chem. Soc.* **2005**, 127, 1644. h) A. W. Kleij, M. Lutz, A. L. Spek, P. W. N. M. van Leeuwen, J. N. H. Reek, *Chem. Commun.* **2005**, 3661. i) I. Yoon, M. Goto, T. Shimizu, S. S. Lee, M. Asakawa, *Dalton Trans.* **2004**, 1513. j) I. Yoon, M. Narita, T. Shimizu, M. Asakawa, *J. Am. Chem. Soc.* **2004**, 126, 16740.
- 55 a) S. Akine, T. Taniguchi, T. Nabeshima, *Tetrahedron Lett.* **2001**, 42, 8861. b) S. Akine, T. Taniguchi, T. Nabeshima, *J. Am. Chem. Soc.* **2006**, 128, 15765.
- 56 a) A. W. Kleij, *Chem.—Eur. J.* **2008**, 14, 10520. b) H. L. C. Feltham, S. Brooker, *Coord. Chem. Rev.* **2009**, 253, 1458.
- 57 S. Akine, T. Taniguchi, T. Nabeshima, *Chem. Lett.* **2001**, 682.
- 58 S. Akine, T. Taniguchi, W. Dong, S. Masubuchi, T. Nabeshima, *J. Org. Chem.* **2005**, 70, 1704.
- 59 S. Akine, S. Sunaga, T. Taniguchi, H. Miyazaki, T. Nabeshima, *Inorg. Chem.* **2007**, 46, 2959.
- 60 a) S. Akine, T. Taniguchi, T. Nabeshima, *Inorg. Chem.* **2004**, 43, 6142. b) S. Akine, T. Nabeshima, *Inorg. Chem.* **2005**, 44, 1205. c) S. Akine, T. Taniguchi, T. Nabeshima, *Chem. Lett.* **2006**, 35, 604. d) S. Akine, W. Dong, T. Nabeshima, *Inorg. Chem.* **2006**, 45, 4677.
- 61 S. Akine, T. Taniguchi, T. Nabeshima, *Angew. Chem., Int. Ed.* **2002**, 41, 4670.
- 62 S. Akine, T. Taniguchi, T. Nabeshima, *Inorg. Chem.* **2008**, 47, 3255.
- 63 S. Akine, T. Taniguchi, T. Saiki, T. Nabeshima, *J. Am. Chem. Soc.* **2005**, 127, 540.
- 64 R. Y. Tsien, *Biochemistry* **1980**, 19, 2396.
- 65 S. Akine, T. Matsumoto, T. Taniguchi, T. Nabeshima, *Inorg. Chem.* **2005**, 44, 3270.
- 66 S. Akine, S. Kagiya, T. Nabeshima, *Inorg. Chem.* **2007**, 46, 9525.

- 67 S. Akine, T. Taniguchi, T. Matsumoto, T. Nabeshima, *Chem. Commun.* **2006**, 4961.
- 68 S. Akine, T. Matsumoto, T. Nabeshima, *Chem. Commun.* **2008**, 4604.
- 69 A. J. Gallant, M. J. MacLachlan, *Angew. Chem., Int. Ed.* **2003**, 42, 5307.
- 70 a) H. Miyazaki, A. Iwasaki, S. Akine, T. Nabeshima, 35th Congress of Heterocyclic Chemistry, Osaka, October 26–28, **2005**, pp. 5–6. b) T. Nabeshima, H. Miyazaki, A. Iwasaki, S. Akine, T. Saiki, C. Ikeda, S. Sato, *Chem. Lett.* **2006**, 35, 1070. c) A. J. Gallant, J. H. Chong, M. J. MacLachlan, *Inorg. Chem.* **2006**, 45, 5248.
- 71 P. D. Frischmann, M. J. MacLachlan, *Chem. Commun.* **2007**, 4480.
- 72 T. Nabeshima, H. Miyazaki, A. Iwasaki, S. Akine, T. Saiki, C. Ikeda, *Tetrahedron* **2007**, 63, 3328.
- 73 T. Nabeshima, N. Tamura, T. Kawazu, K. Sugawara, Y. Yano, *Heterocycles* **1995**, 41, 877.
- 74 T. Nabeshima, T. Takahashi, T. Hanami, A. Kikuchi, T. Kawabe, Y. Yano, *J. Org. Chem.* **1998**, 63, 3802.
- 75 A. Thompson, S. J. Rettig, D. Dolphin, *Chem. Commun.* **1999**, 631.
- 76 S. R. Halper, L. Do, J. R. Stork, S. M. Cohen, *J. Am. Chem. Soc.* **2006**, 128, 15255.
- 77 H. Maeda, M. Hasegawa, T. Hashimoto, T. Kakimoto, S. Nishio, T. Nakanishi, *J. Am. Chem. Soc.* **2006**, 128, 10024.
- 78 J. Chen, J. Reibenspies, A. Derecskei-Kovacs, K. Burgess, *Chem. Commun.* **1999**, 2501.
- 79 C. Ikeda, S. Ueda, T. Nabeshima, *Chem. Commun.* **2009**, 2544.
- 80 C. Ikeda, T. Nabeshima, *Chem. Commun.* **2008**, 721.
- 81 C. Ikeda, N. Sakamoto, T. Nabeshima, *Org. Lett.* **2008**, 10, 4601.
- 82 a) R. Trokowski, S. Akine, T. Nabeshima, *Chem. Commun.* **2008**, 889. b) R. Trokowski, S. Akine, T. Nabeshima, *Dalton Trans.* **2009**, 10359.



Tatsuya Nabeshima was born in 1955 in Kumamoto, Japan. He received his B.S. (1979) from The University of Tokyo, M.S. (1981) from the University of Tsukuba, and Ph.D. degrees (1985) from Kyoto University. In 1985, he joined Stanford University as a postdoctoral fellow. After joining the University of Tsukuba as a research associate in 1986, he became Assistant Professor in 1987. He moved to Gunma University as an assistant professor in 1989 and was promoted to Associate Professor in 1991. He returned to the University of Tsukuba as an associate professor in 1995, and was promoted to Professor in 1999. In 2000 he was a Professor of the Graduate School of Pure and Applied Sciences, University of Tsukuba, and in 2010 he was appointed as Director of Tsukuba Research Center for Interdisciplinary Materials Science (TIMS), University of Tsukuba. His research interests cover artificial receptors, molecular recognition, artificial allosteric and responding molecular systems, and organic–inorganic supramolecular systems. He received The Chemical Society of Japan Award for Creative Work in 2008.